Imprints of relativistic effects on the dipole anisotropy of the density-intrinsic alignment cross-correlation

Shohei Saga
(Paris observatory, LUTH)

Collaborators:
T.Okumura (ASIAA), A.Taruya(YITP), T.Inoue (ASIAA)

Contents

1.1. Galaxy redshift survey

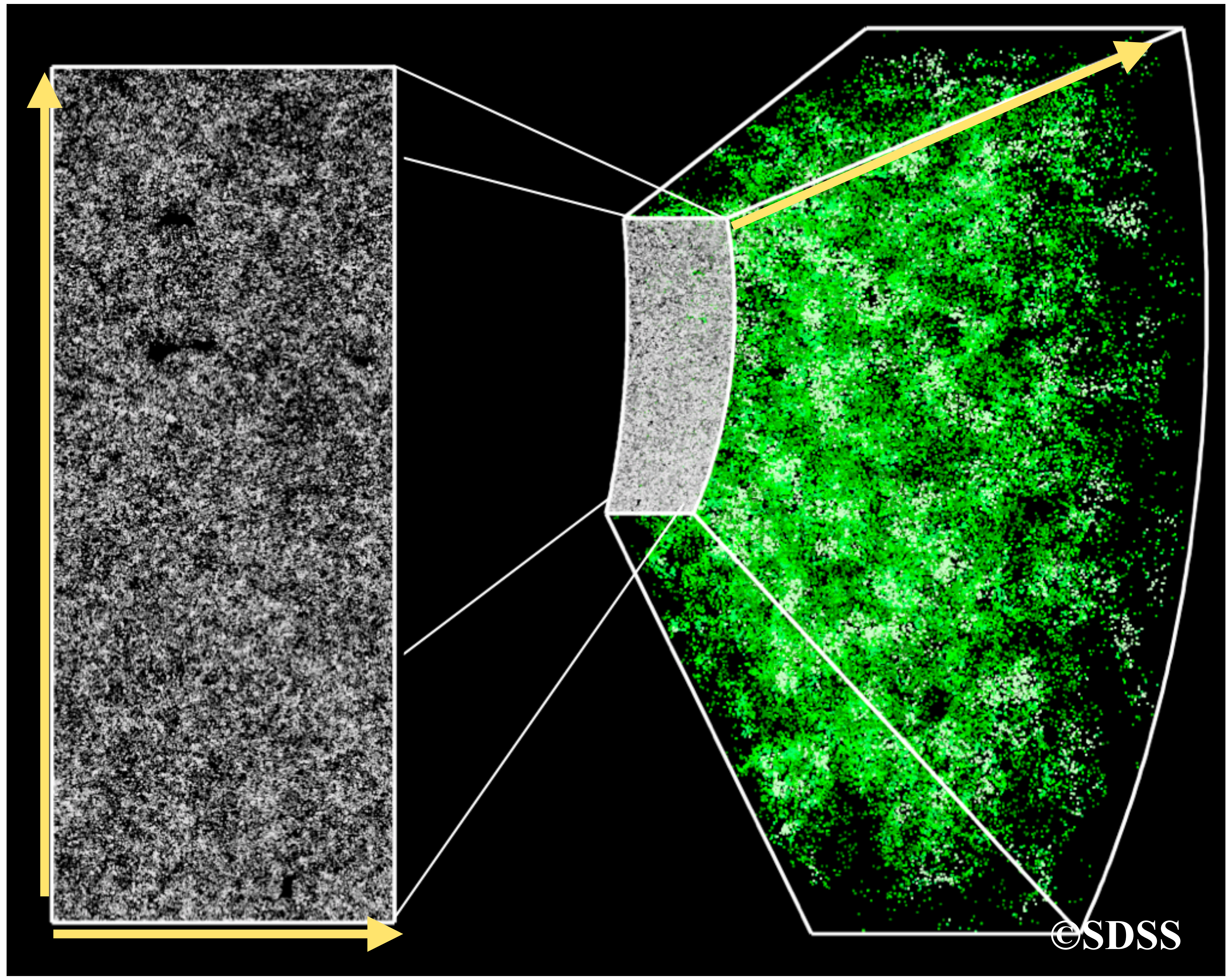

3D map of our universe by measuring

redshift: $z = \dfrac{\lambda_{\rm obs} - \lambda_{em}}{\lambda_{\rm em}}$

angular position: (θ, ϕ)

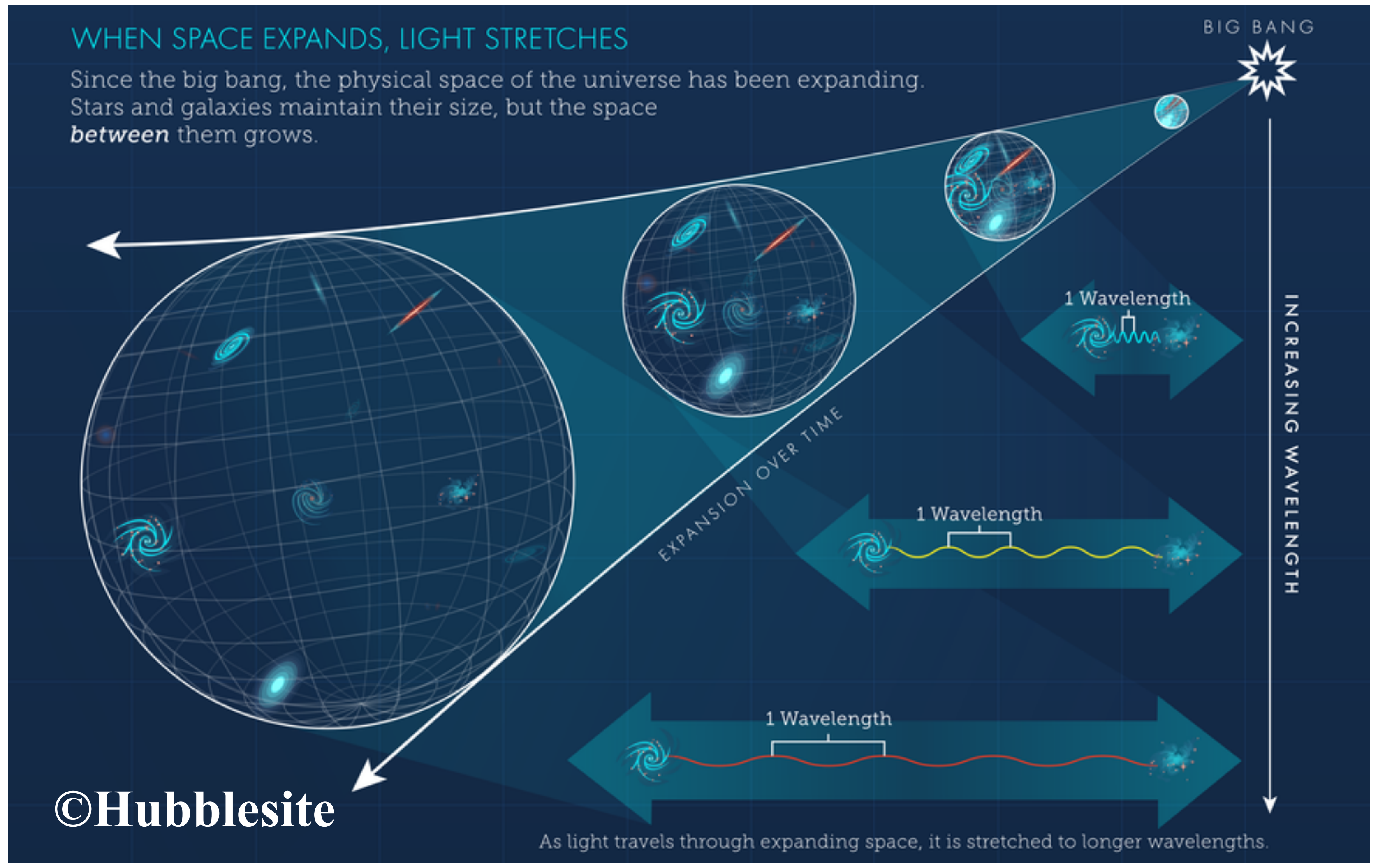

Observed redshift

Cosmological redshift (Hubble flow) + **Doppler effect (peculiar velocity)**

Observed position (inferred from redshift) ≠ Actual position

1.2. Redshift space distortions (RSD)

Observed galaxy distribution appears distorted

↓

Redshift space distortions (RSD)

Primary source: Doppler effect induced by peculiar velocity

Large scale: coherent infall

Real space (Actual position) | **Redshift space (Apparent position)**

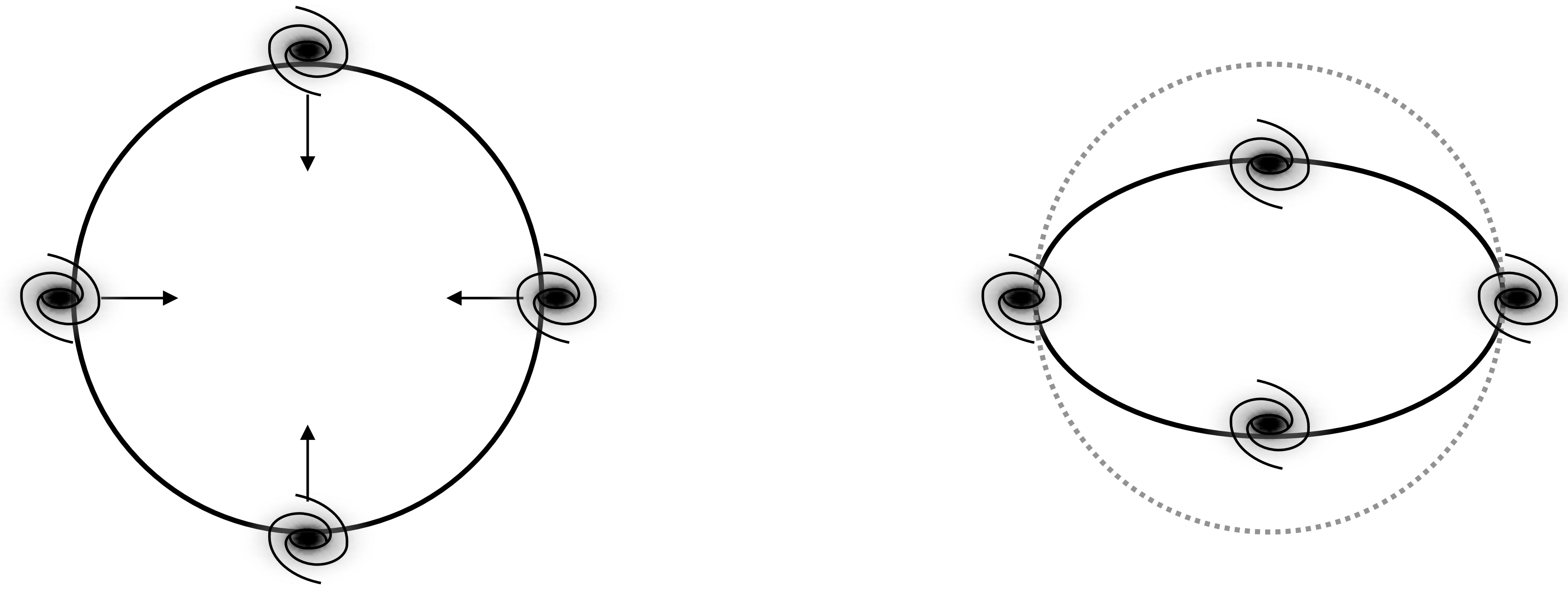

↑ **line-of-sight direction**

Observer

Kaiser effect

Small scale: virial motion

Real space (Actual position) | **Redshift space (Apparent position)**

↑ **line-of-sight direction**

Observer

Finger-of-God effect

1.3 Cosmology - RSD

Redshift space ↔ Real space

N. Kaiser (1987)

redshift space $\boldsymbol{s} = \boldsymbol{r} + \frac{1+z}{H(z)}(\boldsymbol{v}\cdot\hat{\boldsymbol{z}})\,\hat{\boldsymbol{z}}$ special relativity, $v \ll 1$

real space $\hat{z}$: constant line-of-sight vector

continuity equation (linear): $\dot{\delta}_{\rm L} + \frac{1}{a}\nabla\cdot\boldsymbol{v} \simeq 0$

conservation law: $\left(1+\delta^{(\rm s)}(\boldsymbol{s})\right)\mathrm{d}^3 s = \left(1+\delta(\boldsymbol{r})\right)\mathrm{d}^3 r$

Kaiser formula

$$\delta^{(\rm s)}(\boldsymbol{k}) = \left(b + f(\hat{\boldsymbol{k}}\cdot\hat{\boldsymbol{z}})^2\right)\delta_{\rm L}(\boldsymbol{k})$$

$f \equiv \frac{\mathrm{d}\ln\delta_{\rm L}}{\mathrm{d}\ln a}$: linear growth rate

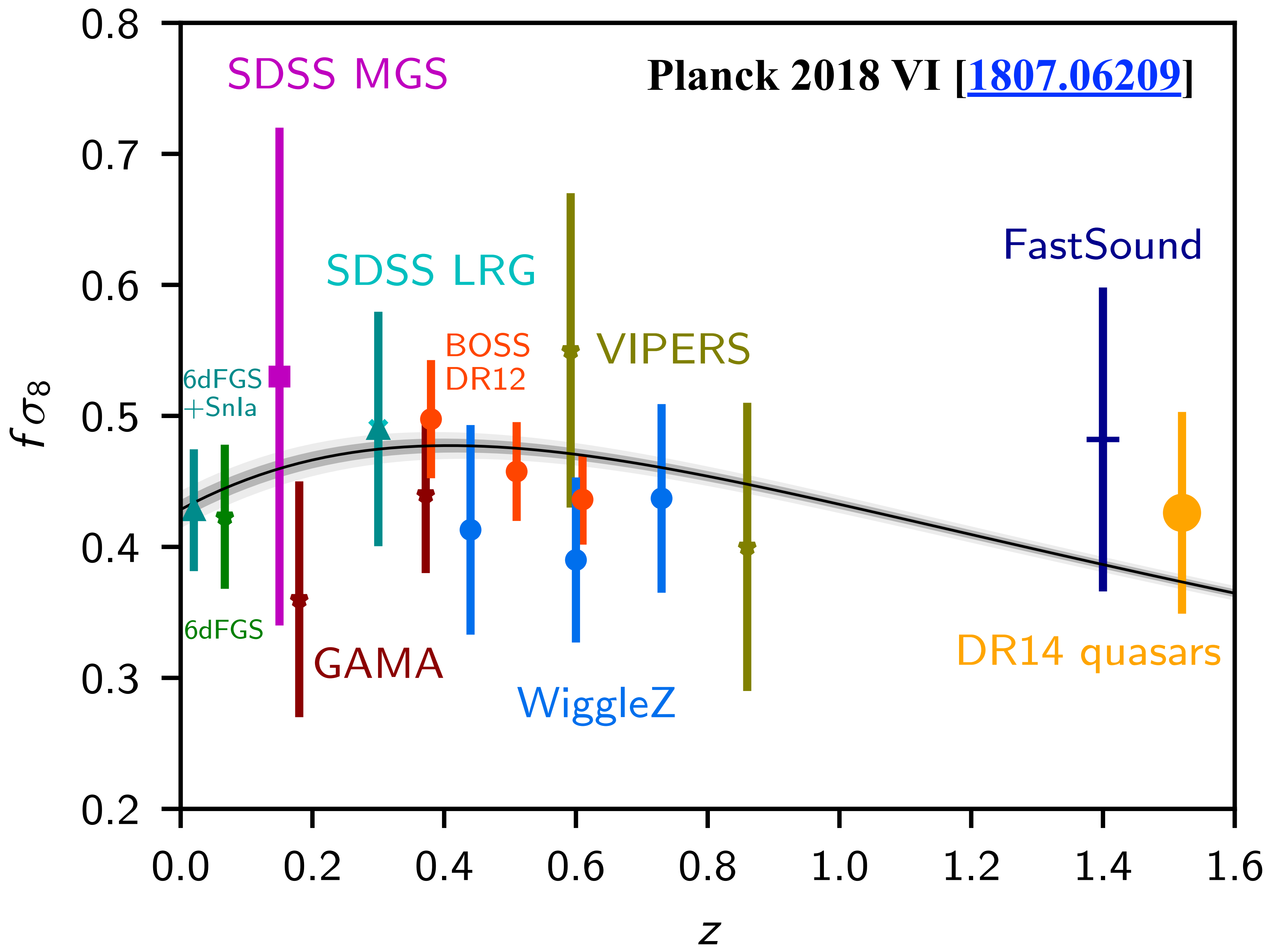

Linear growth rate depends on the gravity theory
→ a **probe of gravity** on cosmological scales

For ΛCDM: $f \approx \left(\Omega_{\rm m}(a)\right)^{0.55}$

1.4. Other relativistic effects

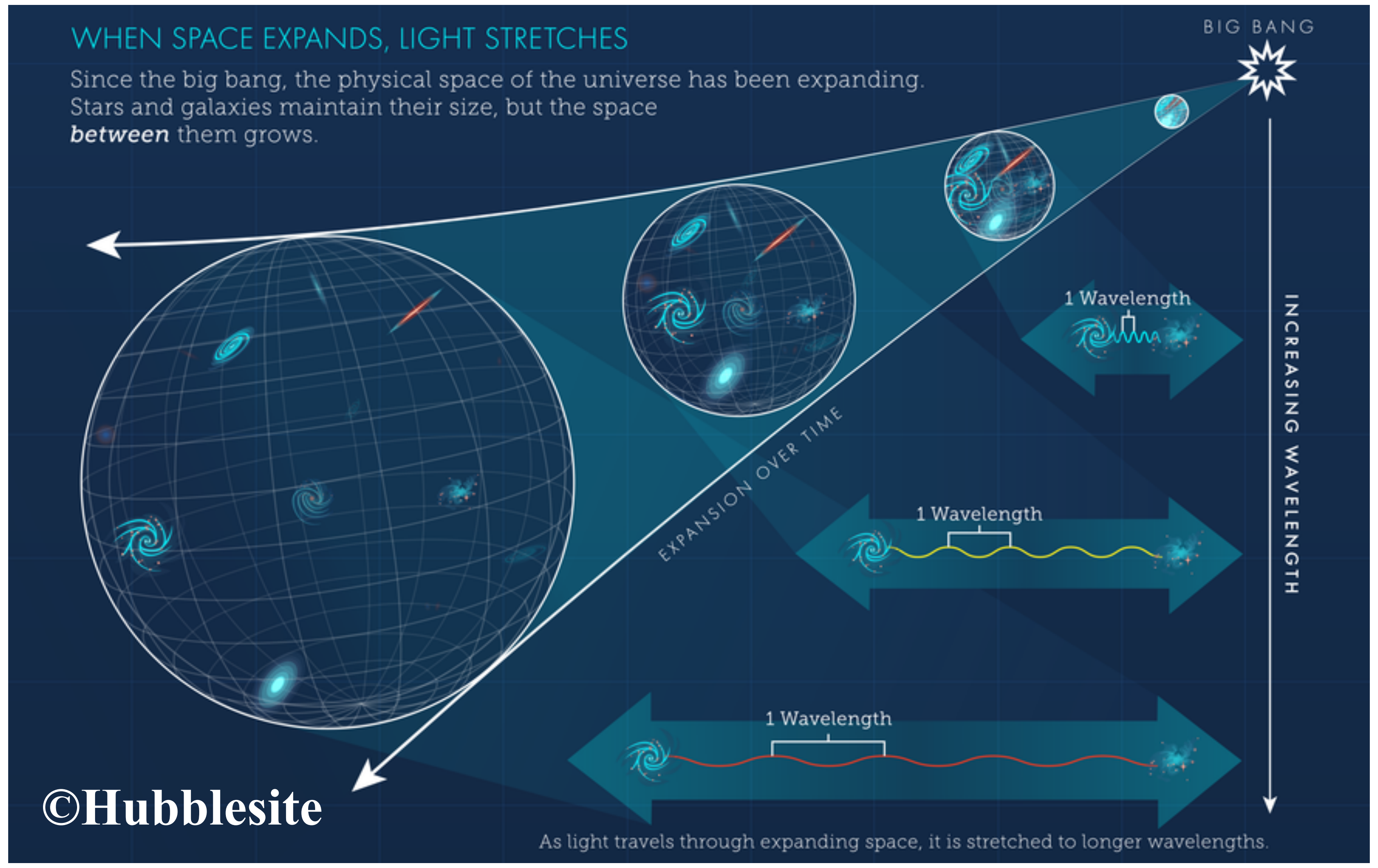

Observed redshift

Cosmological redshift (Hubble flow)

+ **Doppler effect (peculiar velocity)**

Other relativistic effects

+ **Gravitational redshift**
+ **Integrated Sachs-Wolfe**
+ **Shapiro Time delay**
+ **Gravitational lensing**
+ **...**

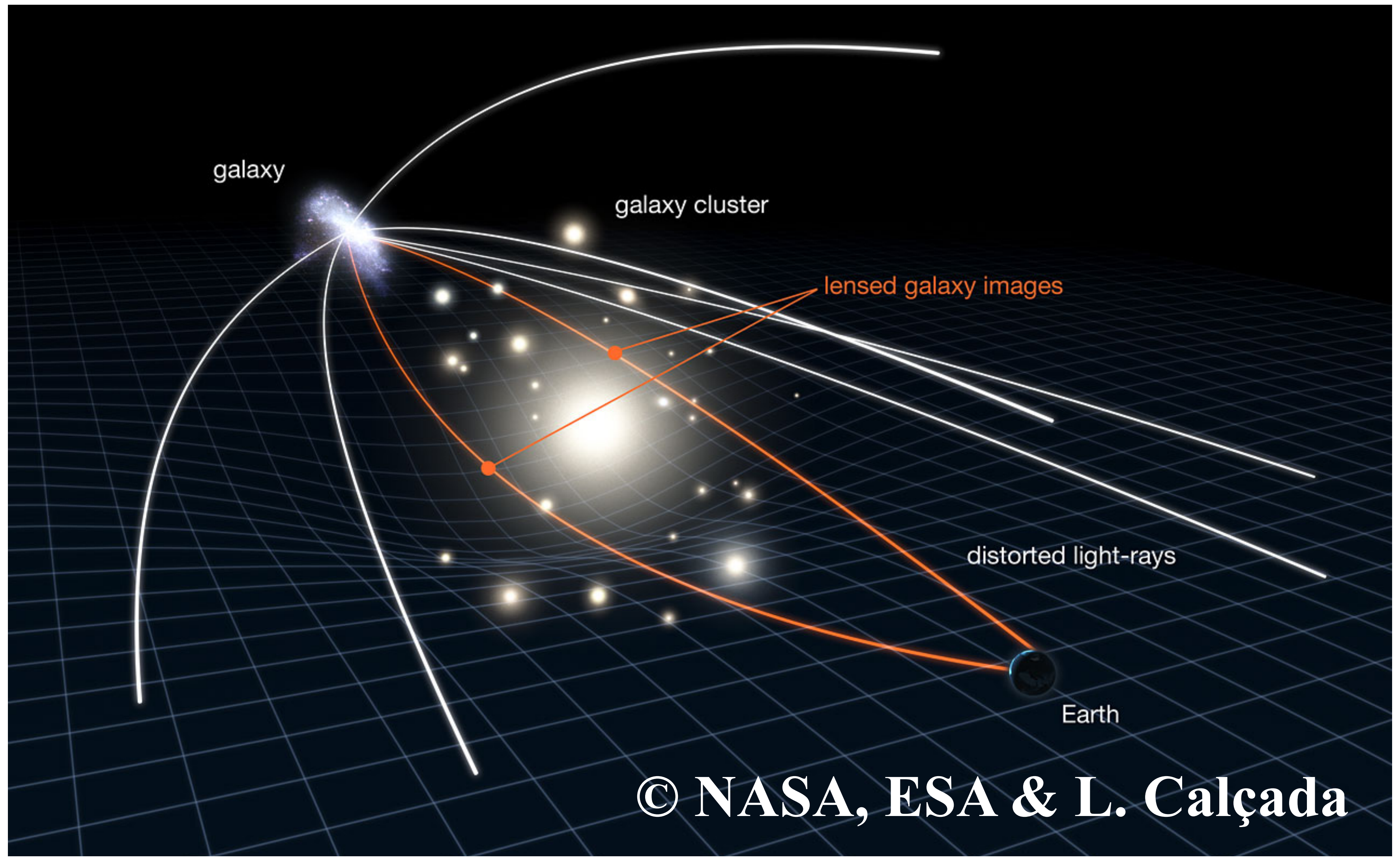

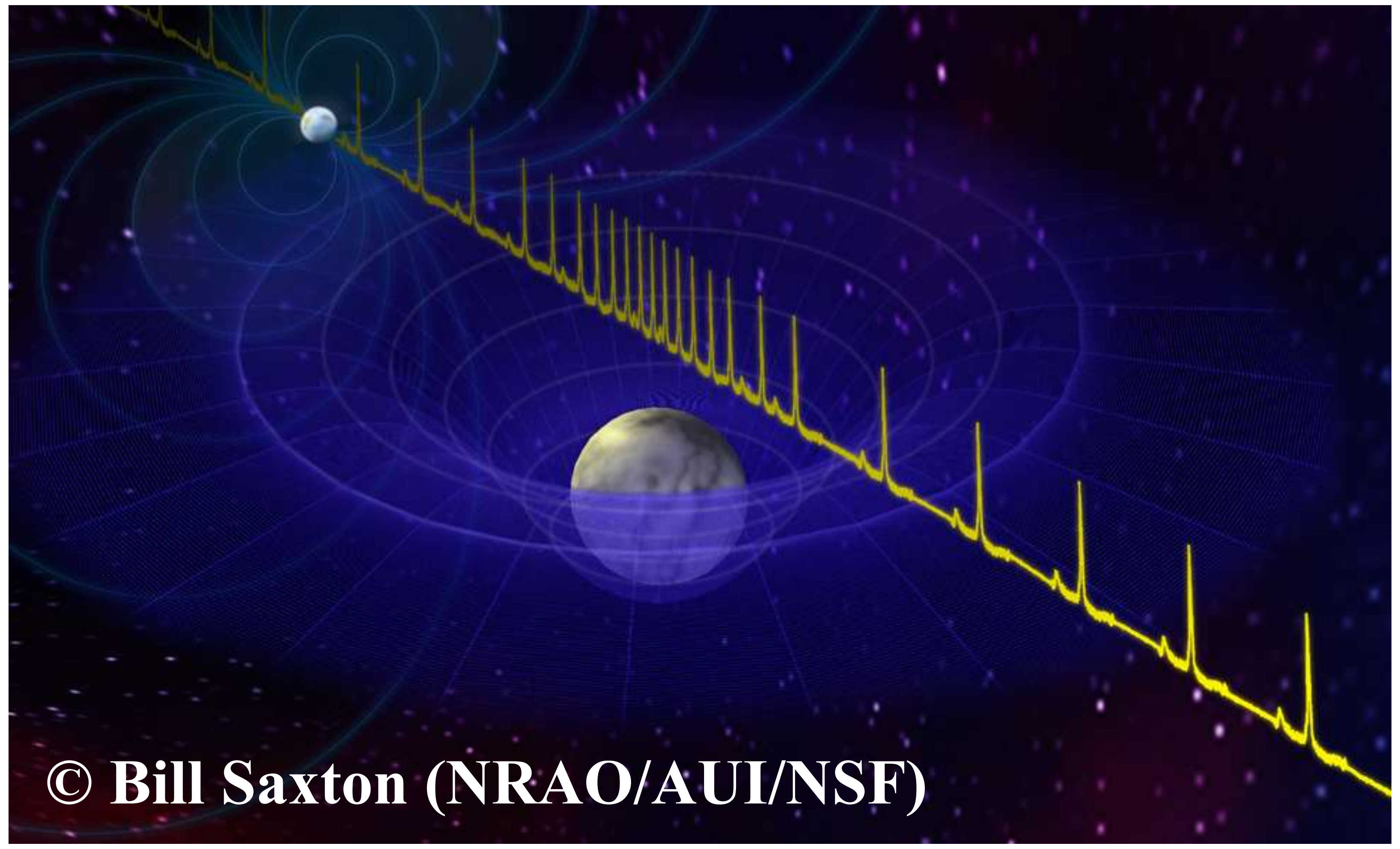

1.5. How is the signal of relativistic effects observed?

A.Challinor and A.Lewis [1105.5292]
C.Bonvin and R.Durrer [1105.5280]
J.Yoo [1409.3223],
and many works

- Perturbed FLRW: $\mathrm{d}s^2 = \left[-(1+2\Phi)\mathrm{d}t^2 + a^2(1-2\Psi)\mathrm{d}x^2\right]$
- Solve the geodesic eq.: $\dfrac{\mathrm{d}k^\mu}{\mathrm{d}\lambda} + \Gamma^\mu_{\alpha\beta}k^\alpha k^\beta = 0$
- Define observed redshift including all effects: $1+z = \dfrac{(k_\mu u^\mu)_\mathrm{S}}{(k_\mu u^\mu)_\mathrm{O}}$

Redshift space including possible relativistic effects

$$\boldsymbol{s} = \boldsymbol{r} + \frac{1+z}{H}(\boldsymbol{v}\cdot\hat{\boldsymbol{r}})\hat{\boldsymbol{r}}$$

$$+\frac{1+z}{H}\left(-\Phi + \frac{1}{2}v^2 - \int_t^{t_0}\left(\dot{\Phi}+\dot{\Psi}\right)\mathrm{d}t'\right)\hat{\boldsymbol{r}} - \int_0^{\chi}(\Psi+\Psi)\mathrm{d}\chi'\,\hat{\boldsymbol{r}} - \int_0^{\chi}(\chi-\chi')\,\nabla_\perp(\Phi+\Psi)\mathrm{d}\chi'$$

- gravitational redshift
- Transverse Doppler

- Shapiro time delay
- integrated Sachs-Wolfe
- gravitational lensing

1.6. How is the signal of relativistic effects observed?

Observed redshift including possible relativistic effects

$$\boldsymbol{s} = \boldsymbol{r} + \frac{1+z}{H}(\boldsymbol{v}\cdot\hat{\boldsymbol{r}})\hat{\boldsymbol{r}}$$
$$+\frac{1+z}{H}\left(-\Phi + \frac{1}{2}v^2 - \int_t^{t_0}\left(\dot{\Phi}+\dot{\Psi}\right)\mathrm{d}t'\right)\hat{\boldsymbol{r}} - \int_0^{\chi}(\Psi+\Psi)\mathrm{d}\chi'\,\hat{\boldsymbol{r}} - \int_0^{\chi}(\chi-\chi')\nabla_{\perp}(\Phi+\Psi)\mathrm{d}\chi'$$

c.f. Kaiser formula

conservation law: $\left(1+\delta^{(\mathrm{S})}(s)\right)\mathrm{d}^3s = \left(1+\delta(r)\right)\mathrm{d}^3r$

(linear approximation)

Linear density field with relativistic effects

(line-of-sight vectors are highlighted in red)

$$\delta^{(\mathrm{s})} = b\delta - \frac{1}{\mathcal{H}}\hat{\boldsymbol{r}}\cdot\frac{\partial}{\partial\boldsymbol{r}}(\hat{\boldsymbol{r}}\cdot\boldsymbol{v})$$
$$-\left(\frac{2}{r\mathcal{H}}+\frac{\dot{\mathcal{H}}}{\mathcal{H}^2}\right)\hat{\boldsymbol{r}}\cdot\boldsymbol{v} + \frac{1}{\mathcal{H}}\left(\hat{\boldsymbol{r}}\cdot\frac{\partial}{\partial\boldsymbol{r}}\Psi + \mathcal{H}\hat{\boldsymbol{r}}\cdot\boldsymbol{v} + \hat{\boldsymbol{r}}\cdot\dot{\boldsymbol{v}}\right)$$
$$-2\Phi + \Psi + \frac{\dot{\Phi}}{\mathcal{H}} + \frac{1}{r}\int_0^r \mathrm{d}r'\left(2 - \frac{r-r'}{r'}\Delta_{\Omega}\right)(\Phi+\Psi) + \left(\frac{2}{r\mathcal{H}}+\frac{\dot{\mathcal{H}}}{\mathcal{H}^2}\right)\left(\Psi + \int_0^r \mathrm{d}r'\left(\dot{\Psi}+\dot{\Phi}\right)\right)$$

Using this expression, we can intuitively understand how we will observe

1.7. Recalling Kaiser effect

Large scale: coherent infall

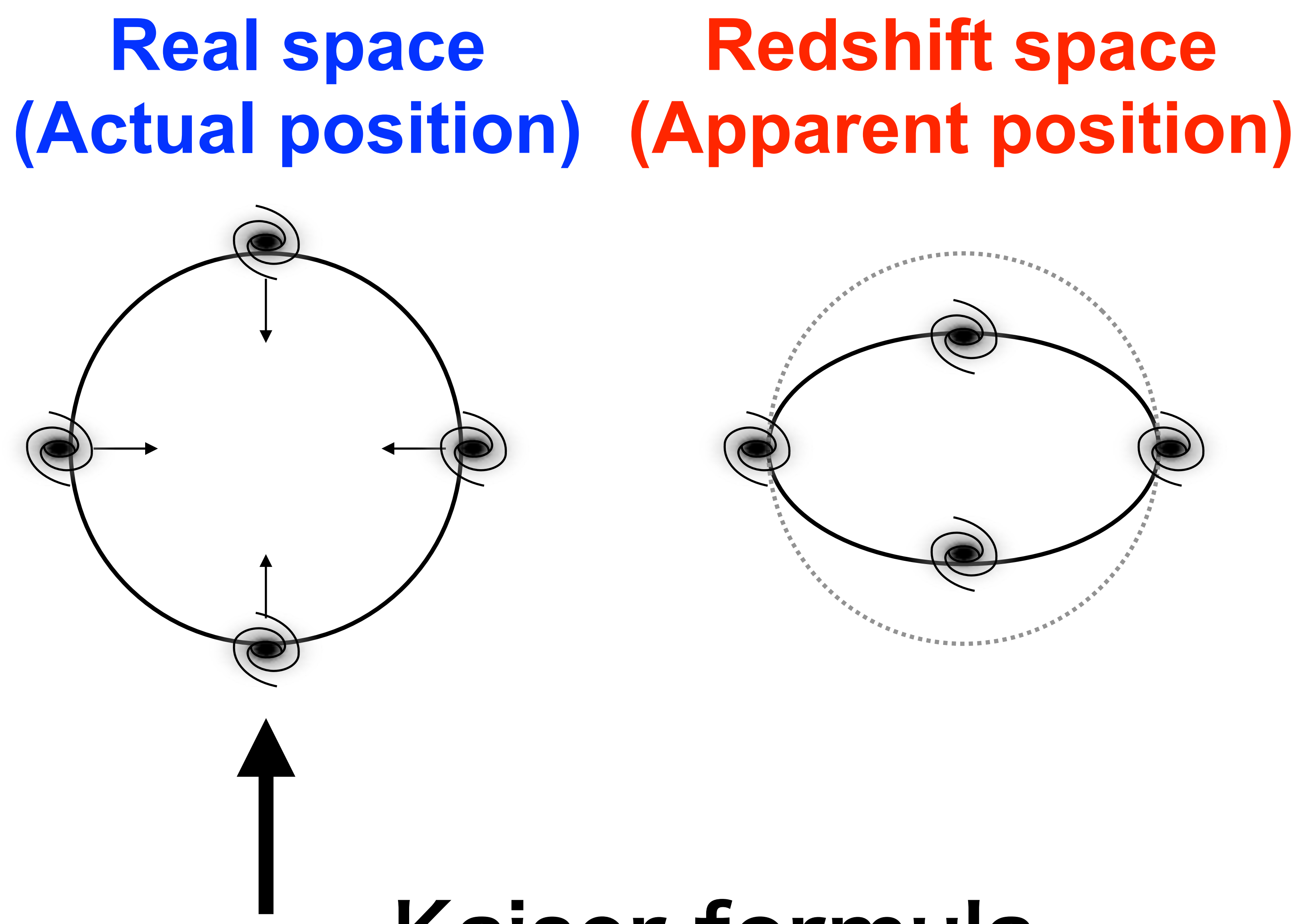

Kaiser formula

$$\delta^{(\mathrm{s})}(\boldsymbol{k}) = \left(b + f(\hat{\boldsymbol{k}} \cdot \hat{z})^2\right) \delta_{\mathrm{L}}(\boldsymbol{k})$$

1.7. Recalling Kaiser effect

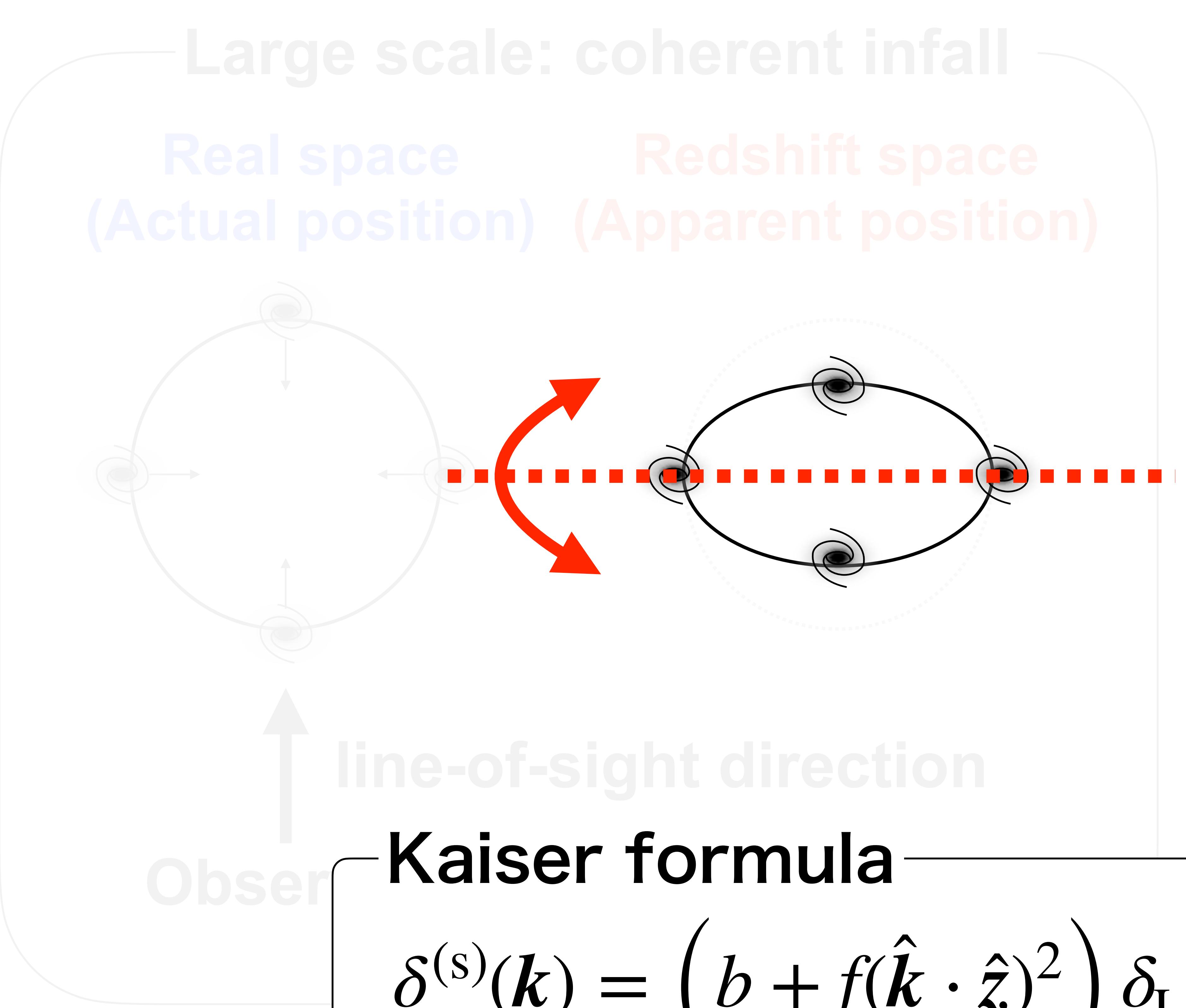

Kaiser formula

$$\delta^{(\mathrm{s})}(\boldsymbol{k}) = \left(b + f(\hat{\boldsymbol{k}}\cdot\hat{z})^2\right)\delta_{\mathrm{L}}(\boldsymbol{k})$$

(line-of-sight vector)^2
→ even multipole anisotropies

1.7. Recalling Kaiser effect

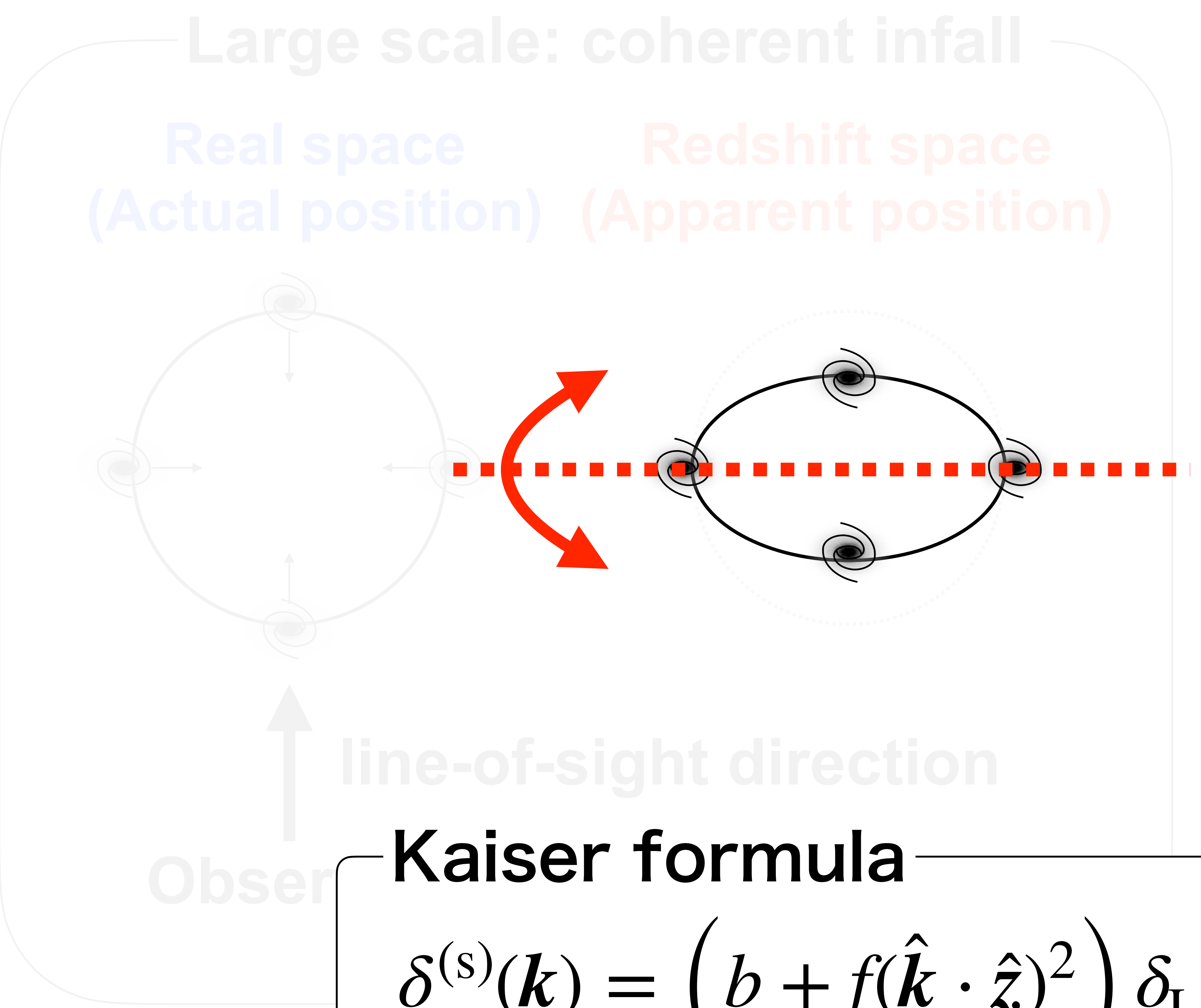

Kaiser formula

$$\delta^{(\mathrm{s})}(\boldsymbol{k}) = \left(b + f(\hat{\boldsymbol{k}}\cdot\hat{z})^2\right)\delta_{\mathrm{L}}(\boldsymbol{k})$$

(line-of-sight vector)²
→ even multipole anisotropies

With relativistic effects

$$\delta^{(\mathrm{s})} = b\delta - \frac{1}{\mathcal{H}}\hat{\boldsymbol{r}}\cdot\frac{\partial}{\partial\boldsymbol{r}}(\hat{\boldsymbol{r}}\cdot\boldsymbol{v})$$
$$-\left(\frac{2}{r\mathcal{H}} + \frac{\dot{\mathcal{H}}}{\mathcal{H}^2}\right)\hat{\boldsymbol{r}}\cdot\boldsymbol{v} + \frac{1}{\mathcal{H}}\left(\hat{\boldsymbol{r}}\cdot\frac{\partial}{\partial\boldsymbol{r}}\Psi + \mathcal{H}\hat{\boldsymbol{r}}\cdot\boldsymbol{v} + \hat{\boldsymbol{r}}\cdot\dot{\boldsymbol{v}}\right)$$
$$-2\Phi + \Psi + \frac{\dot{\Phi}}{\mathcal{H}} + \frac{1}{r}\int_0^r \mathrm{d}r'\left(2 - \frac{r-r'}{r'}\Delta_\Omega\right)(\Phi+\Psi) + \left(\frac{2}{r\mathcal{H}} + \frac{\dot{\mathcal{H}}}{\mathcal{H}^2}\right)\left(\cdots\right.$$

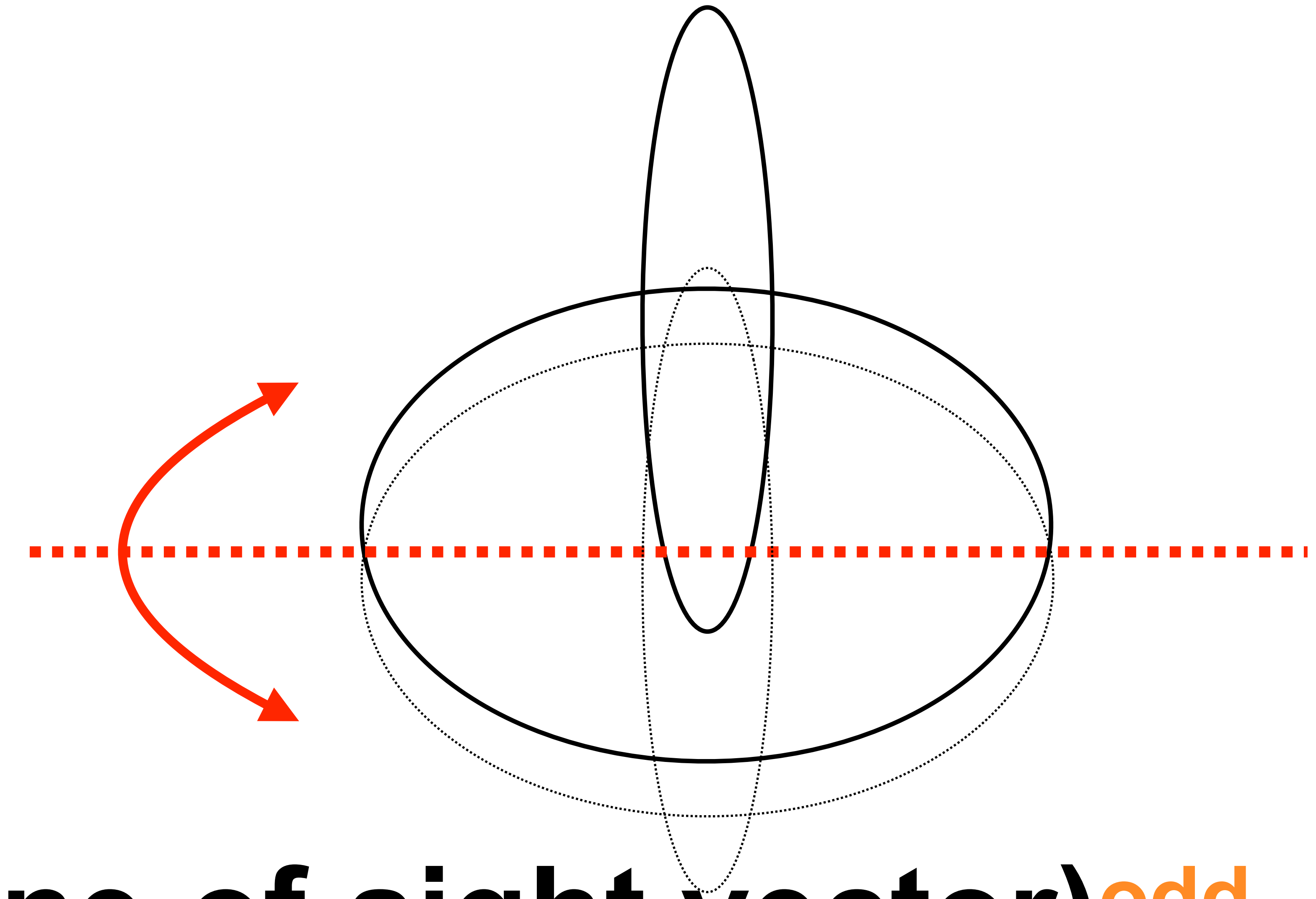

(line-of-sight vector)$^{\mathrm{odd}}$
→ odd multipole anisotropies

Dipole anisotropy

Contents

2.1. Dipole anisotropy

$$\xi_1 = \frac{3}{2}\int_{-1}^{1} \left(\xi^{(\mathrm{S})}(s_1, s_2)\ \cos\theta\right) \mathrm{d}\cos\theta$$

Linear theory: $\xi_1 \propto (b_{\mathrm{X}} - b_{\mathrm{Y}})$

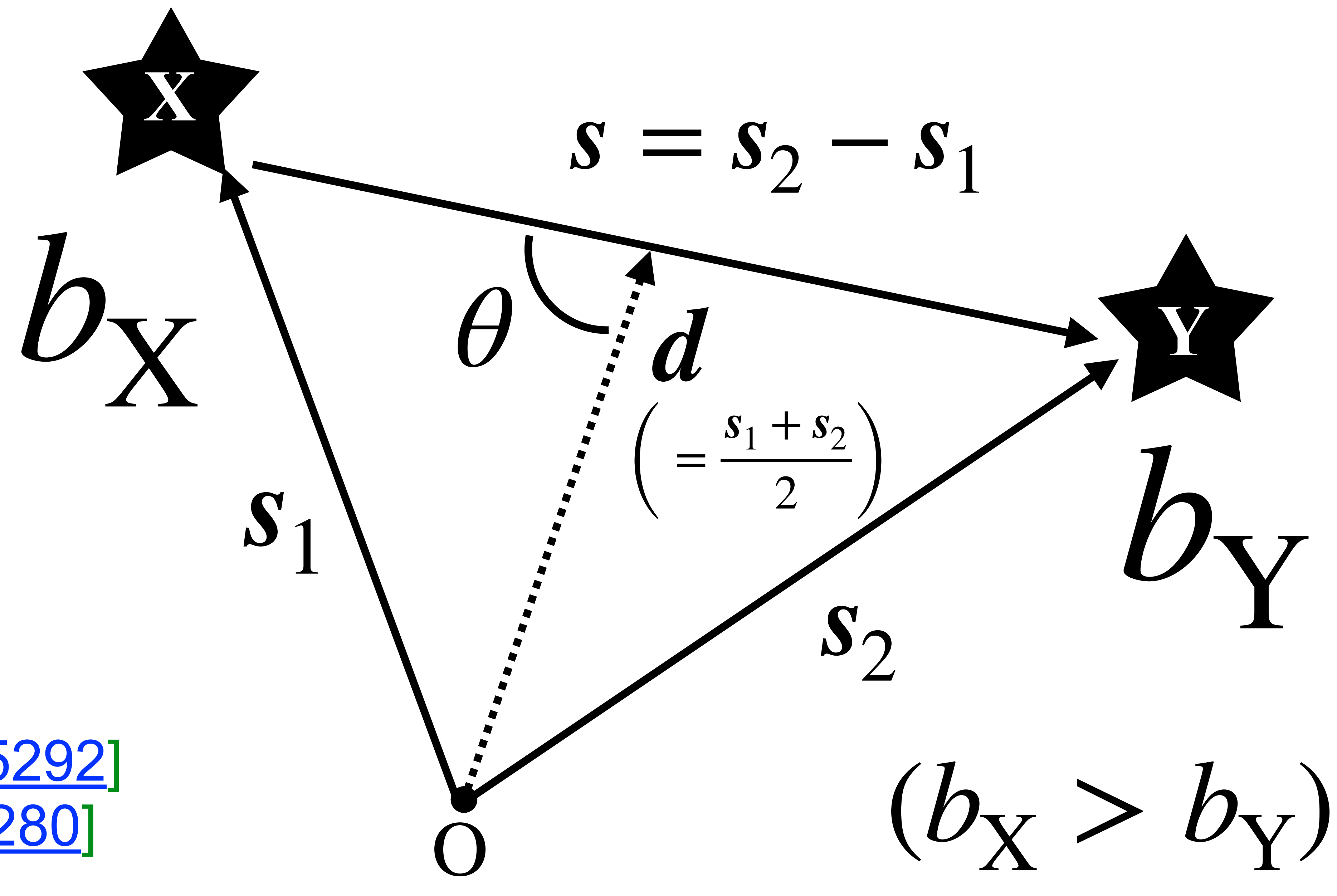

A.Challinor and A.Lewis [1105.5292]
C.Bonvin and R.Durrer [1105.5280]
J.Yoo [1409.3223], ...

Note: wide-angle effect

Beyond the distant-observer limit, the Doppler effect induces non-zero dipole:

$$\boldsymbol{s} = \boldsymbol{r} + \frac{1+z}{H(z)}\left(\boldsymbol{v}\cdot\hat{z}\right)\hat{z}$$

$\hat{z}$: ~~constant~~ line-of-sight vector $\longrightarrow$ $\xi_1 \propto (b_{\mathrm{X}} - b_{\mathrm{Y}})$

Cross-correlating different biased objects is essential

2.2. Dipole in simulations

M-A.Breton, Y.Rasera, A.Taruya, O.Lacombe, S.Saga [1803.04294]

- Using cosmological N-body code RAMSES.
- Storing gravitational potential data on light cone
- Tracing back the light ray to the source by direct integration of geodesic equation
- We obtain "Observed" position and redshift

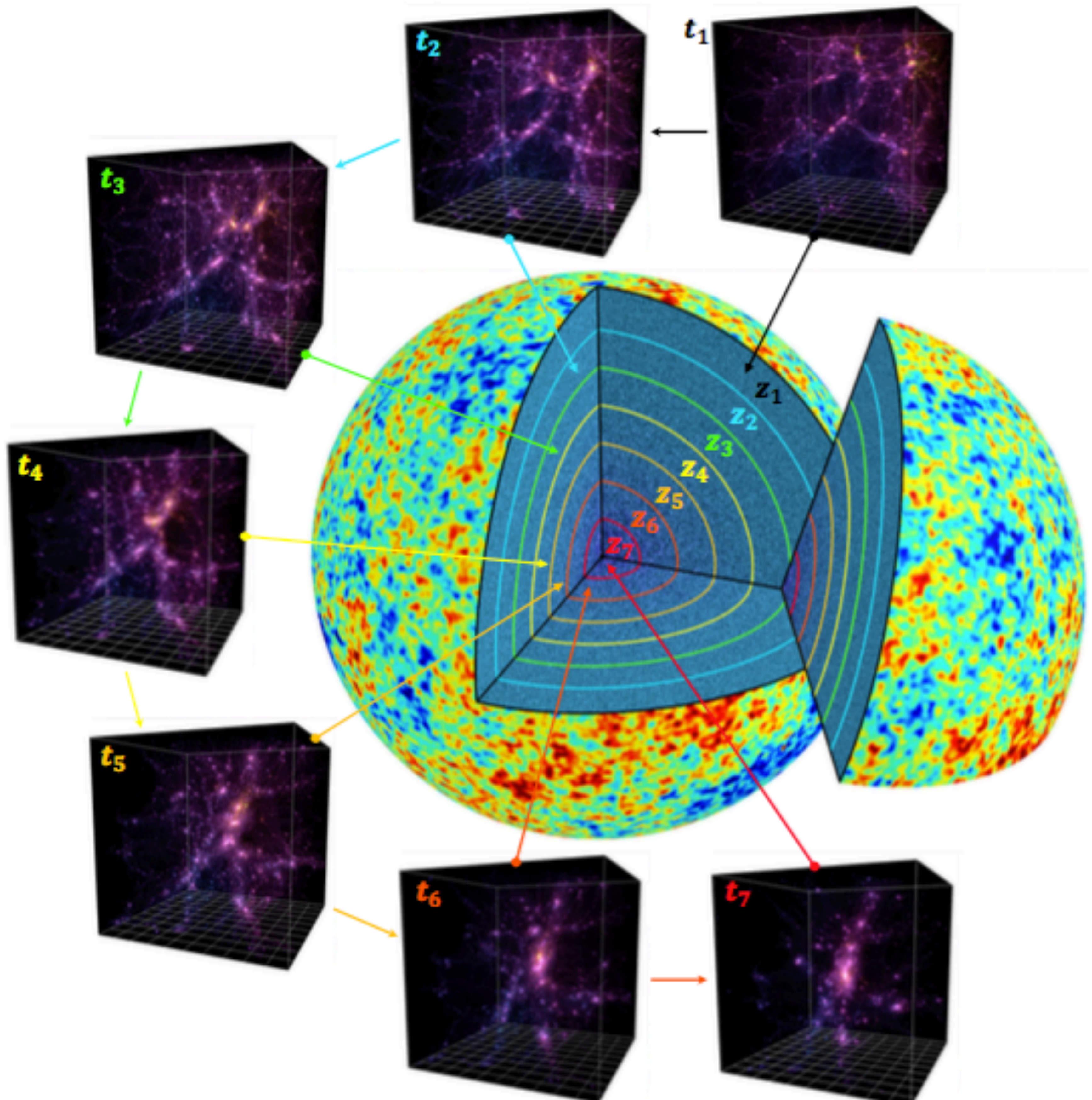

$$1+z=\frac{\left(g_{\mu\nu}k^\mu k^\nu\right)_{\rm source}}{\left(g_{\mu\nu}k^\mu k^\nu\right)_{\rm observer}}$$

$$g_{\mu\nu}k^\mu k^\nu=-ak^0\left(1+\phi+\boldsymbol{v}\cdot\hat{\boldsymbol{n}}+\frac{1}{2}v^2\right)$$

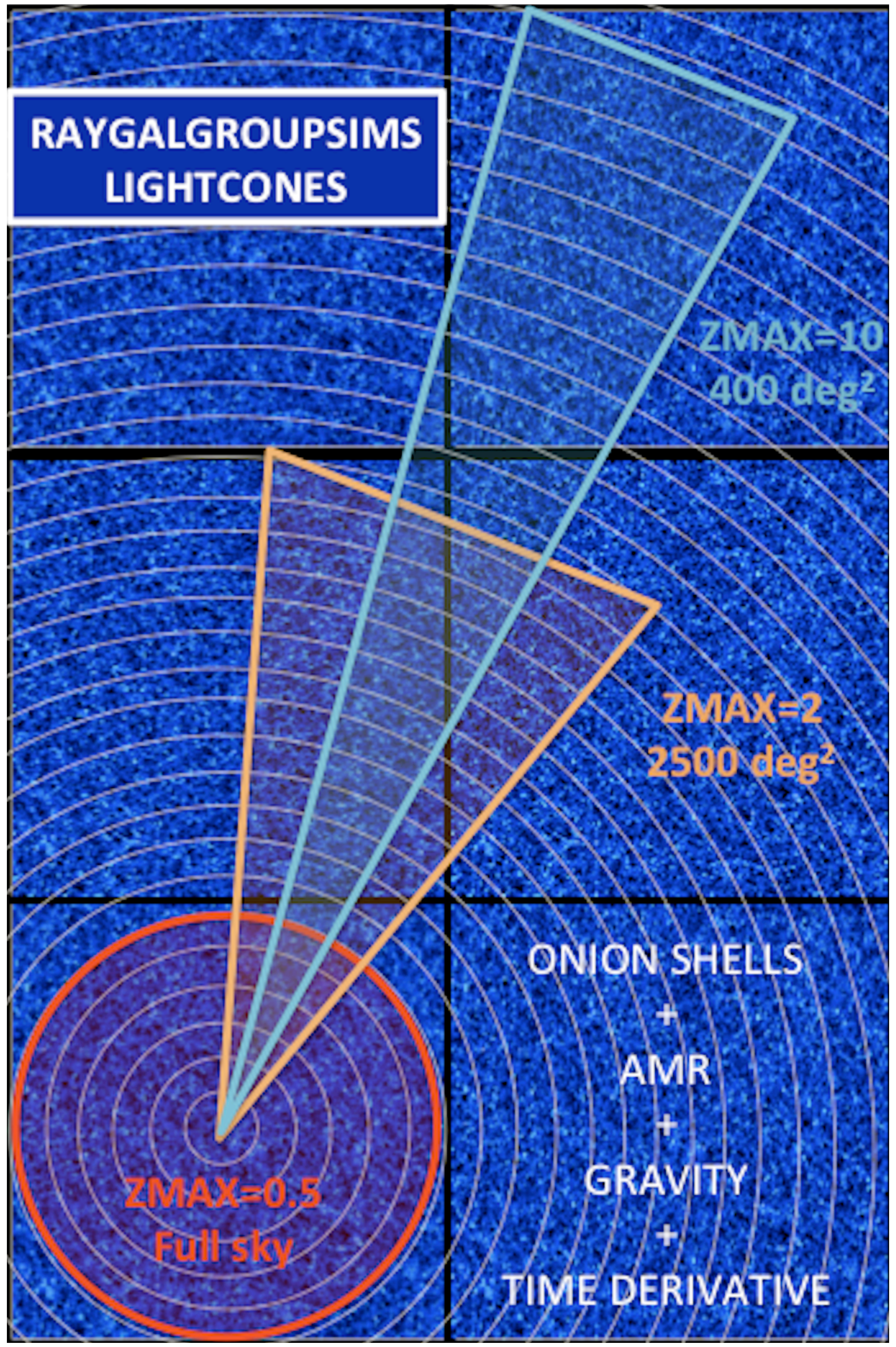

(RayGalGroupSims by M-A.Breton and Y.Rasera)

Light-cone catalogue with all relativistic effects

2.3. Measurements in simulations

M-A.Breton, Y.Rasera, A.Taruya, O.Lacombe, S.Saga [1803.04294]

Large scales

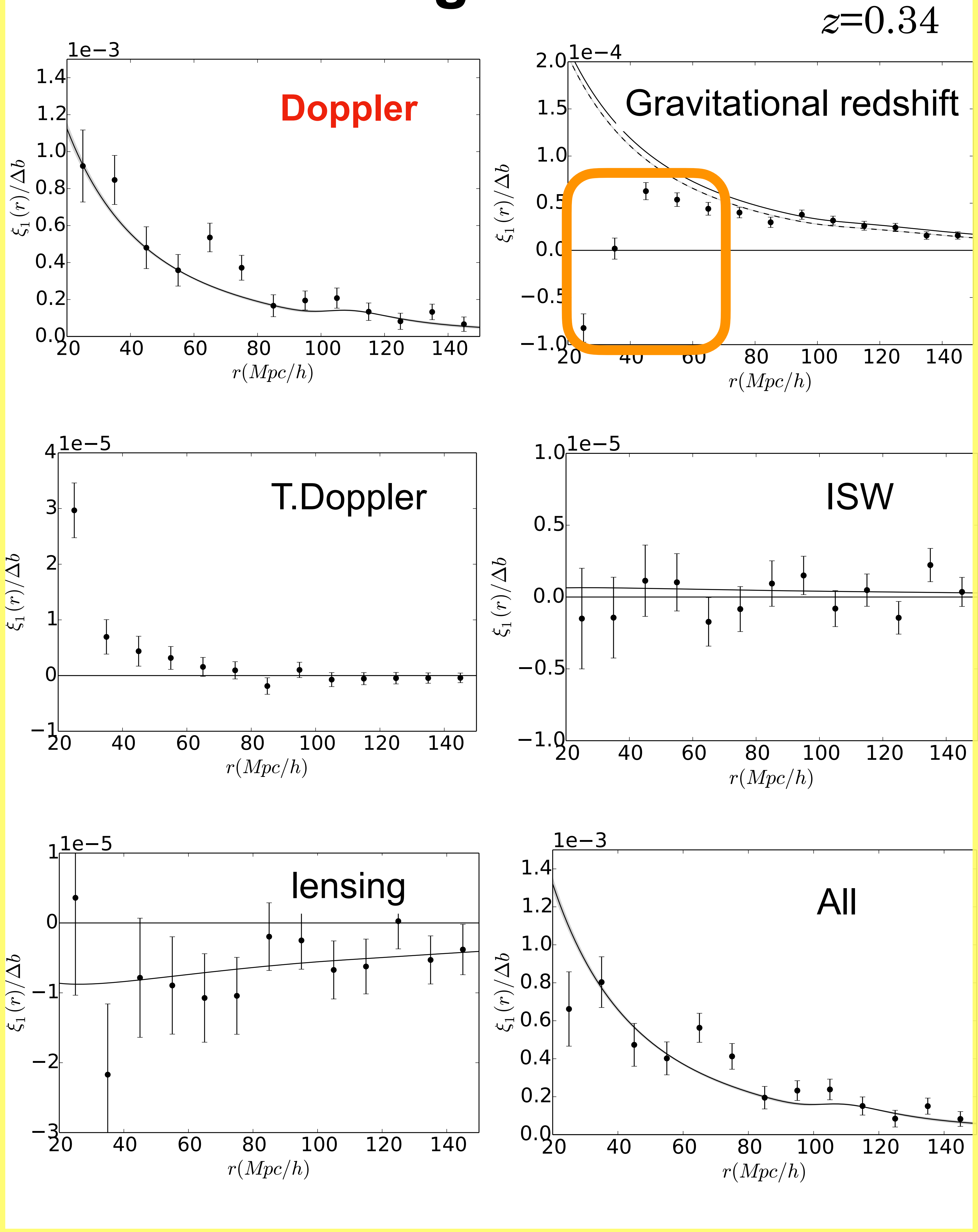

Small scales

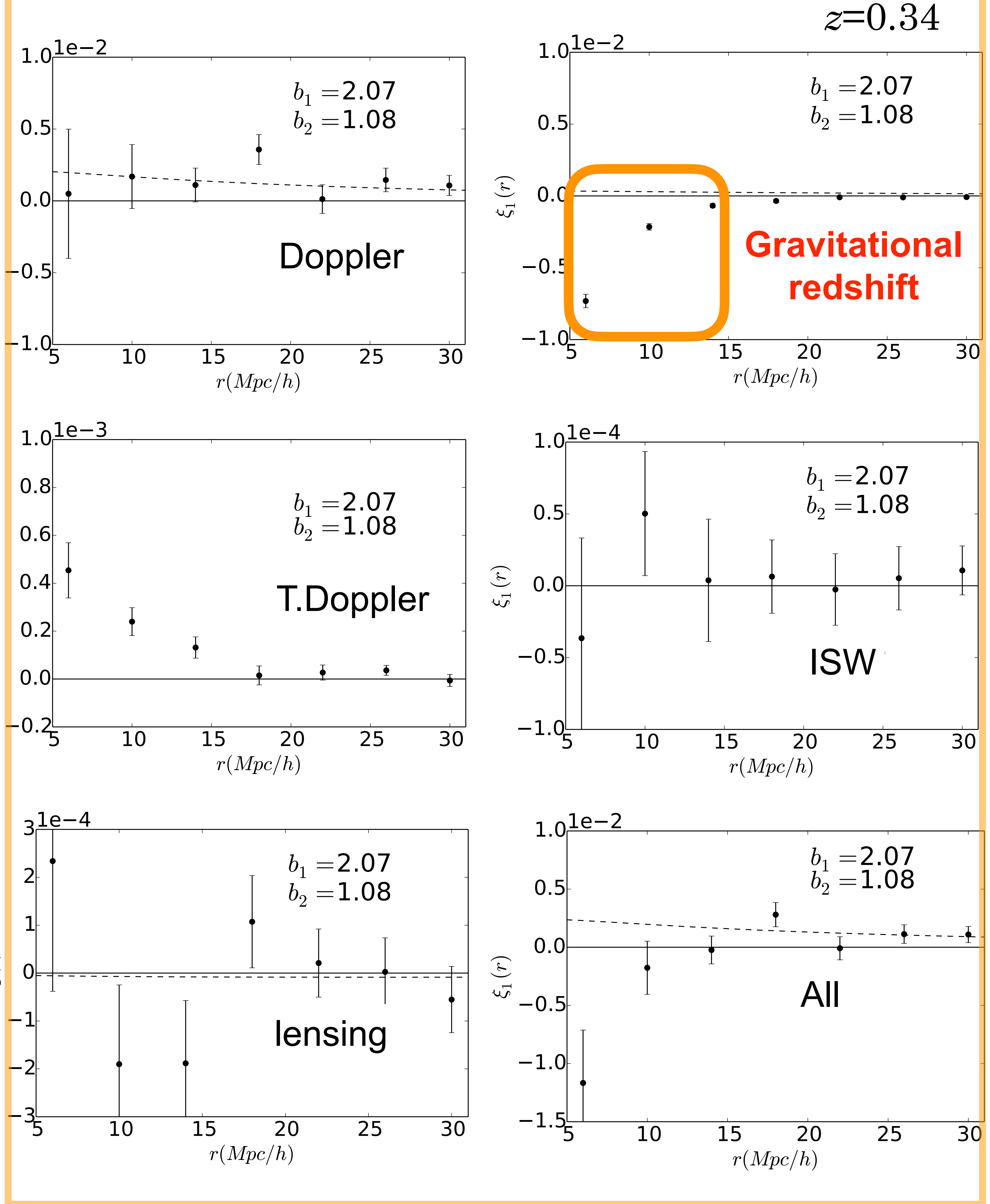

2.4. Our model

S.Saga, A.Taruya, M-A.Breton, Y.Rasera [2004.03772]

Picking up dominant contributions:

$$\boldsymbol{s} = \boldsymbol{r} + \frac{1+z}{H}(\boldsymbol{v}\cdot\hat{\boldsymbol{r}})\hat{\boldsymbol{r}} + \frac{1+z}{H}\left(-\Phi + \frac{1}{2}v^2 - \int_t^{t_0}\left(\dot{\Phi}+\dot{\Psi}\right)dt'\right)\hat{\boldsymbol{r}} - \int_0^{\chi}(\Psi+\Psi)d\chi'\,\hat{\boldsymbol{r}} - \int_0^{\chi}(\chi-\chi')\nabla_\perp(\Phi+\Psi)d\chi'$$

Modelling the potential

$$\Phi = \Phi_{\rm L} + \Phi_{\rm NL}$$

Linear potential

Non-linear halo potential

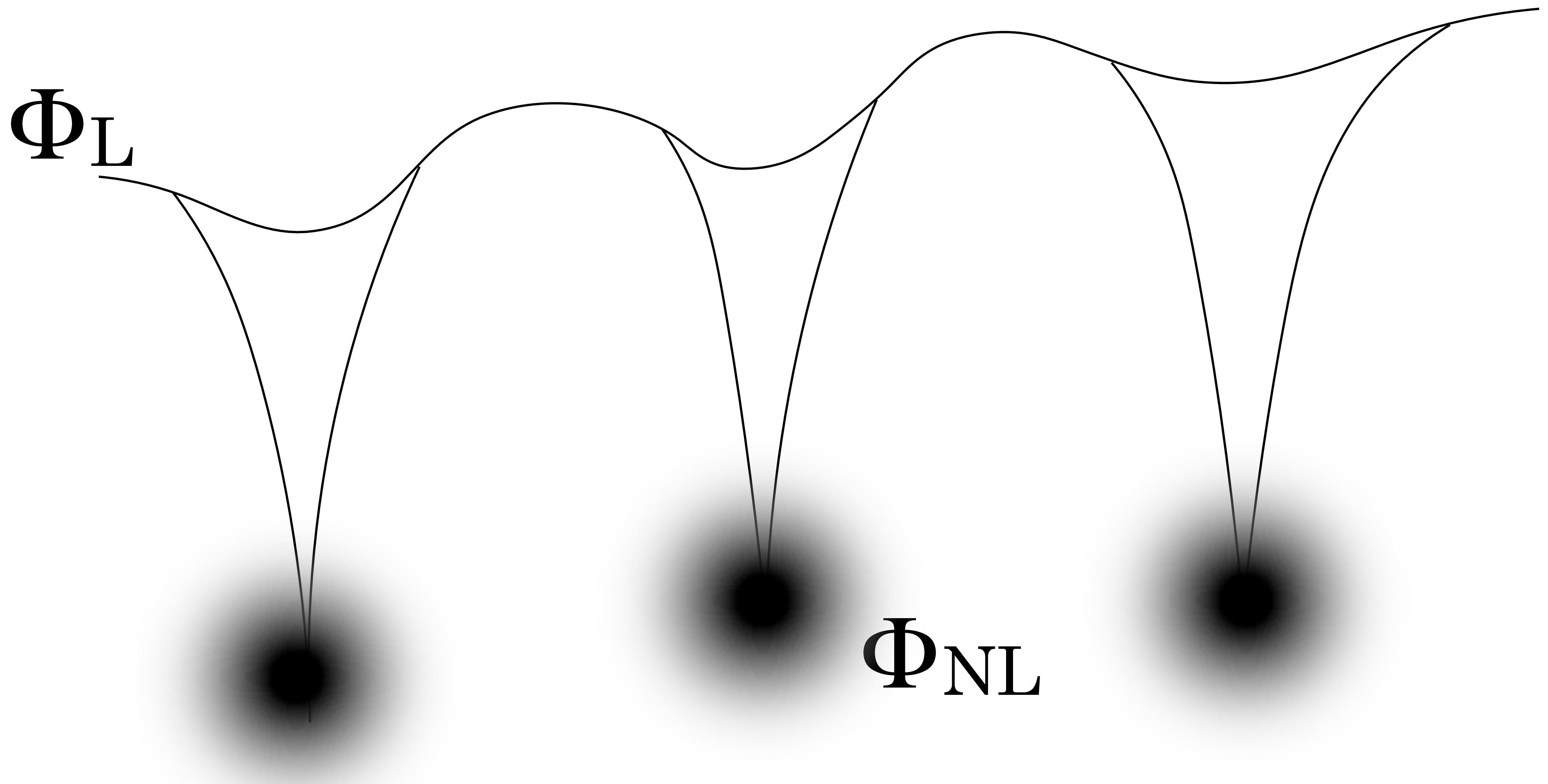

$\Phi_{\rm NL}$ is estimated by NFW profile

δ(std) = Real space + Doppler effect $\equiv \int \frac{d^3\boldsymbol{k}}{(2\pi)^3} e^{i\boldsymbol{k}\cdot\boldsymbol{s}}\left[b + f\mu_k^2 - if\frac{2}{ks}\mu_k\right]\delta_{\rm L}(\boldsymbol{k})\,,$

$\mathcal{M} \equiv -3\Omega_{\rm m0}H_0^2/(2a^2H)$

δ(pot) = Linear potential $\equiv \int \frac{d^3\boldsymbol{k}}{(2\pi)^3} e^{i\boldsymbol{k}\cdot\boldsymbol{s}}\left[(iks\mu_k + 2)\frac{\mathcal{M}}{sk^2}\right]\delta_{\rm L}(\boldsymbol{k})\,,$

δ(NL) = NL potential $\equiv -\frac{\Phi_{\rm NL}}{aHs}\int \frac{d^3\boldsymbol{k}}{(2\pi)^3} e^{i\boldsymbol{k}\cdot\boldsymbol{s}}\left[-1 + (1-2f)\mu_k^2 - i(1+f)\frac{2}{ks}\mu_k - ibks\mu_k - ifks\mu_k^3\right]\delta_{\rm L}(\boldsymbol{k})\,,$

2.5. Dipole in the galaxy-galaxy correlations

$$\xi_{\rm XY}^{\rm (std)} = \langle \delta_{\rm X}^{\rm (std)}(s_1)\delta_{\rm Y}^{\rm (std)}(s_2)\rangle$$

$$\xi_{\rm XY}^{\rm (pot)} = \langle \delta_{\rm X}^{\rm (std)}(s_1)\delta_{\rm Y}^{\rm (pot)}(s_2)\rangle + {\rm X} \leftrightarrow {\rm Y}$$

$$\xi_{\rm XY}^{\rm (NL)} = \langle \delta_{\rm X}^{\rm (std)}(s_1)\delta_{\rm Y}^{\rm (NL)}(s_2)\rangle + {\rm X} \leftrightarrow {\rm Y}$$

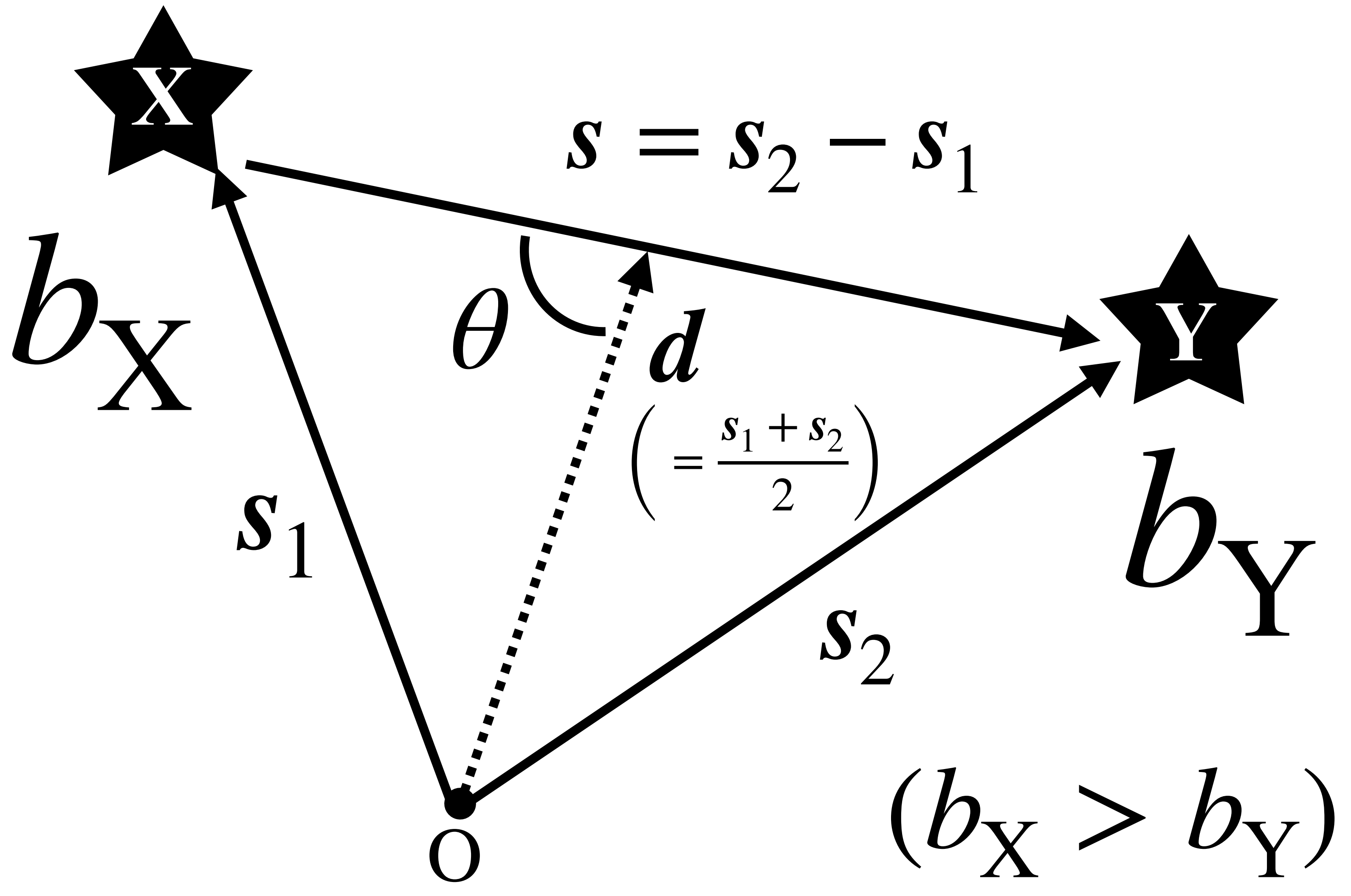

Small scale

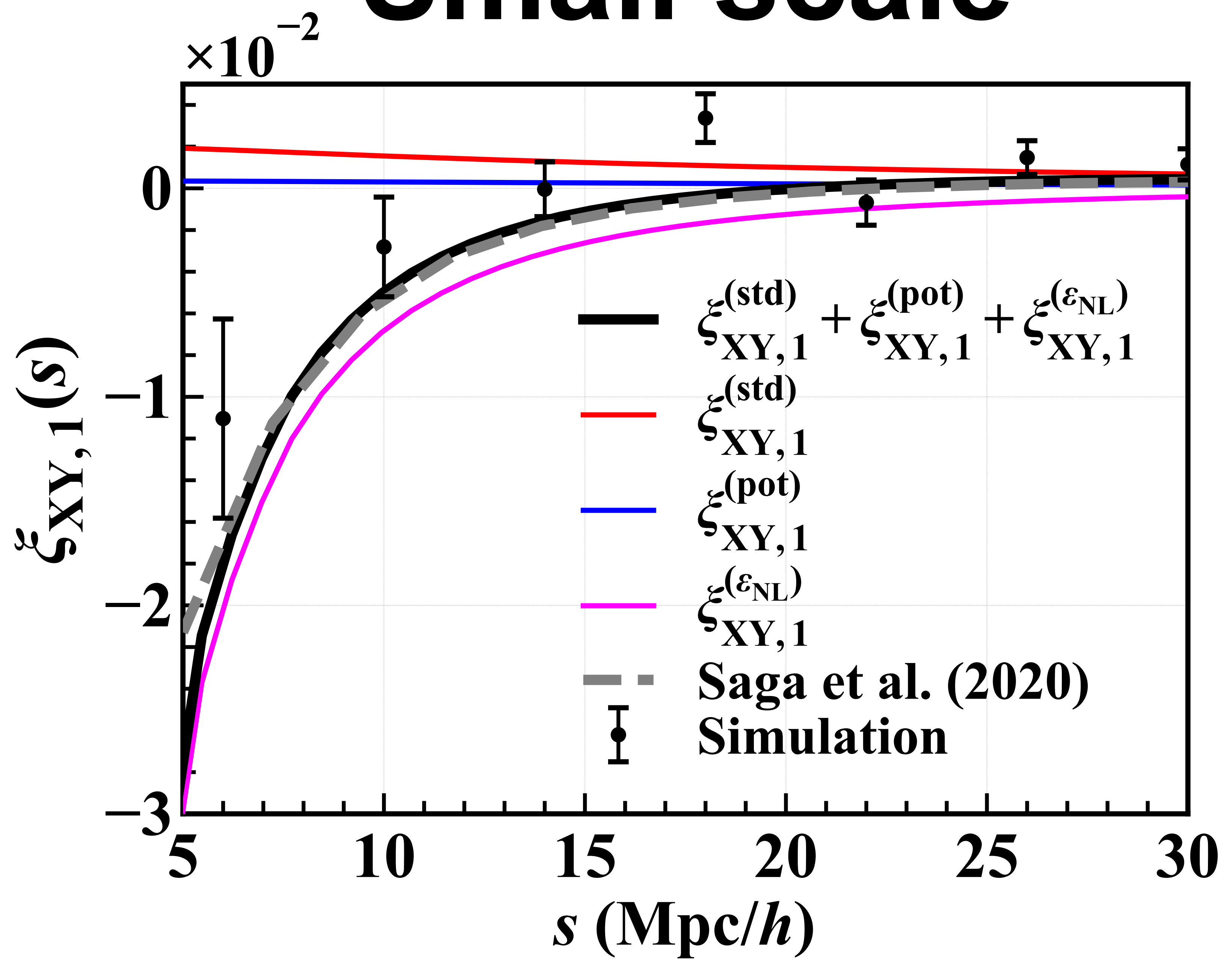

Large scale

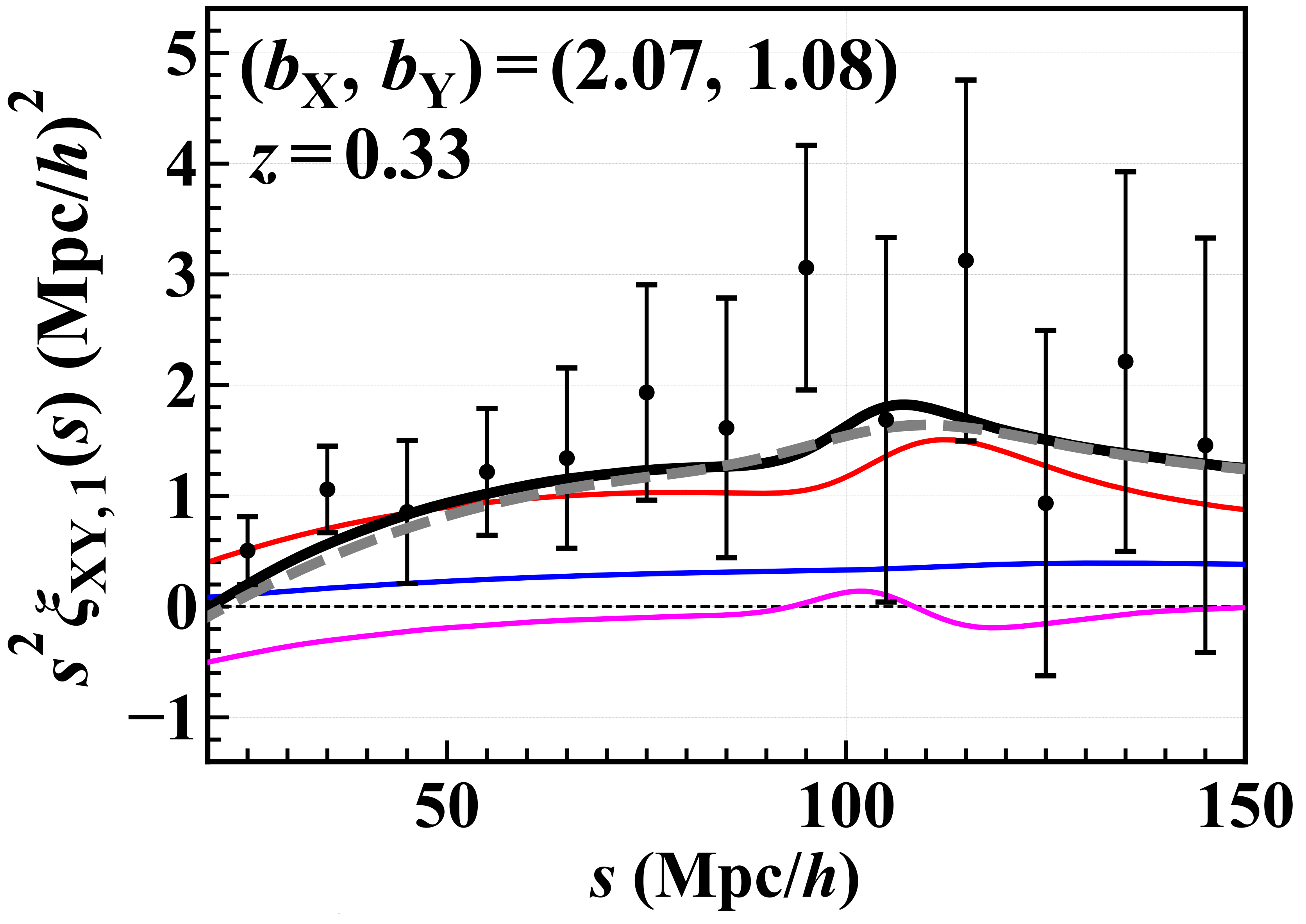

2.6. Recent detection of the dipole

S. Alam et al. [1709.07855]

2.8σ detection of relativistic effects in SDSS DR12 CMASS galaxy sample

- **765,433 LRGs**
- **0.44 < z < 0.70**
- **using the absolute magnitude of galaxies to separate into different biased samples**

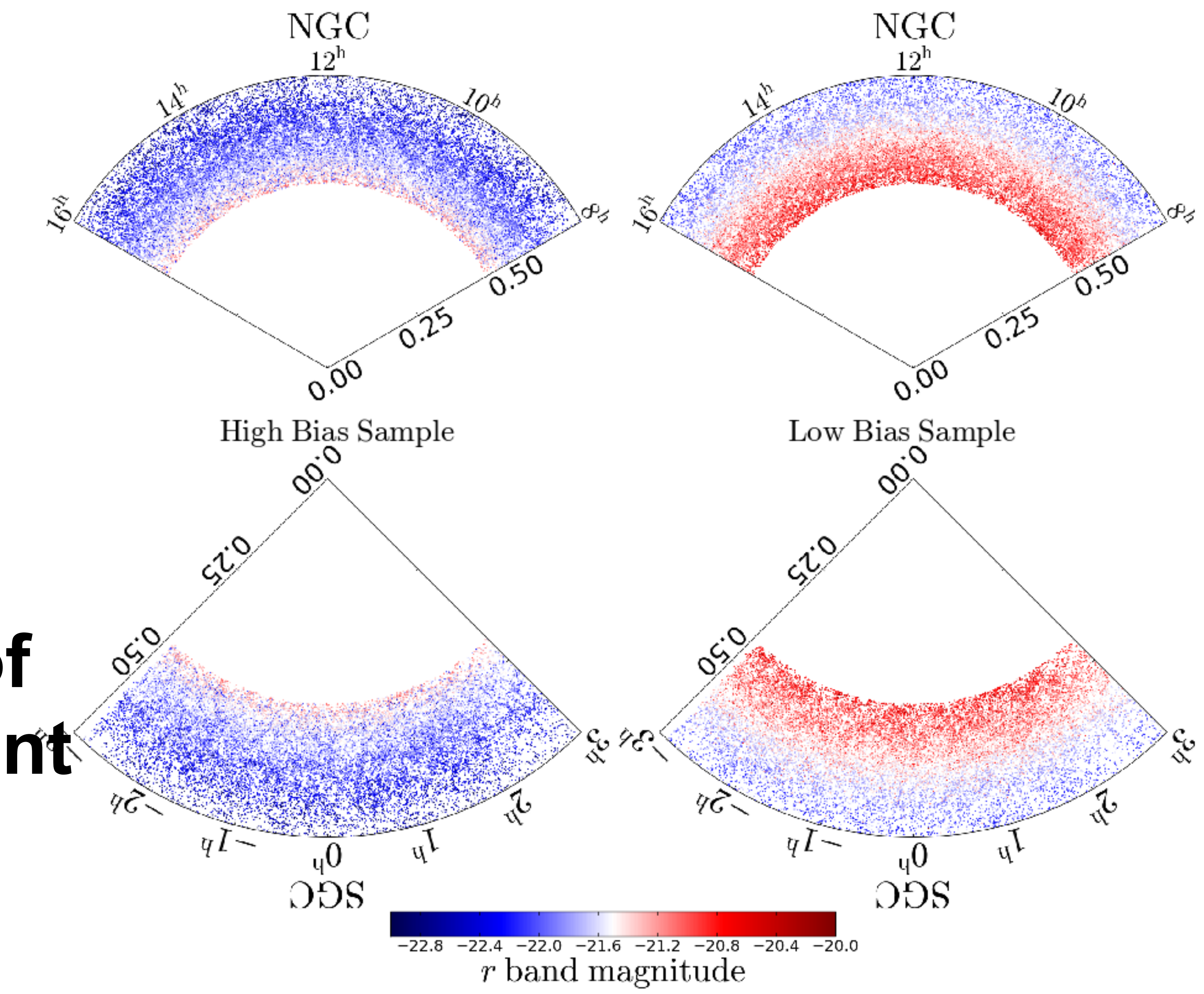

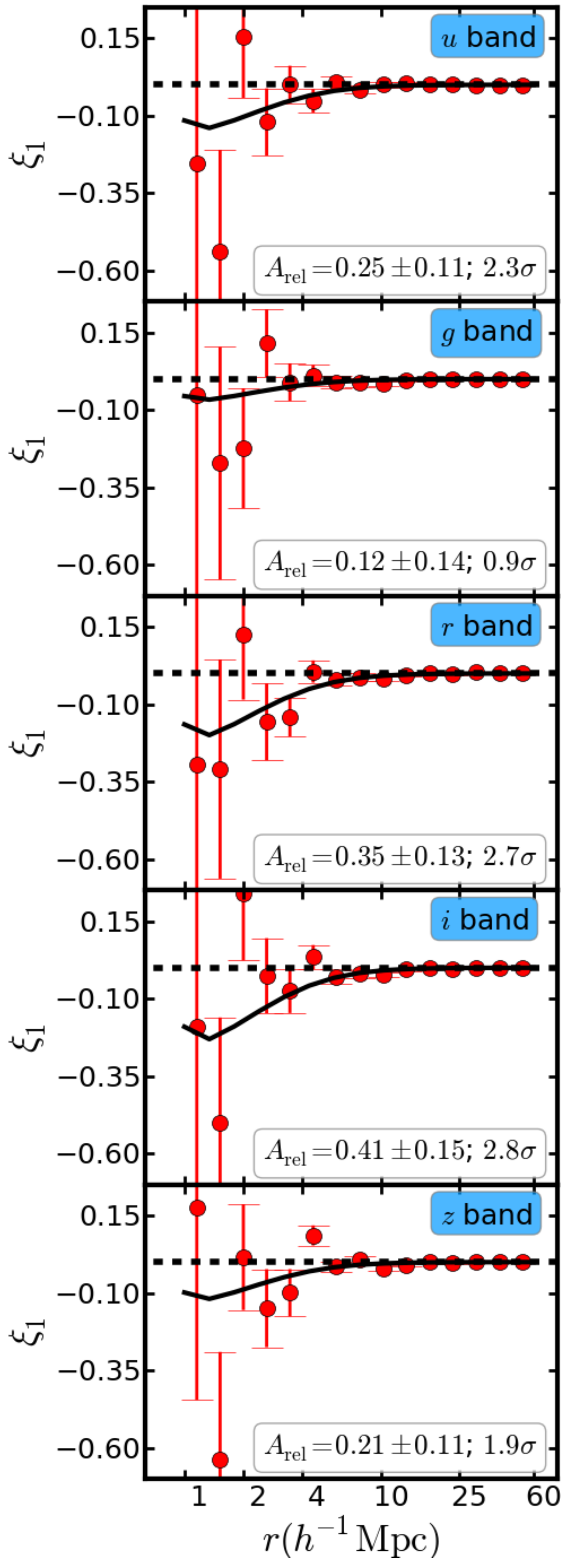

Deep & Wide future surveys

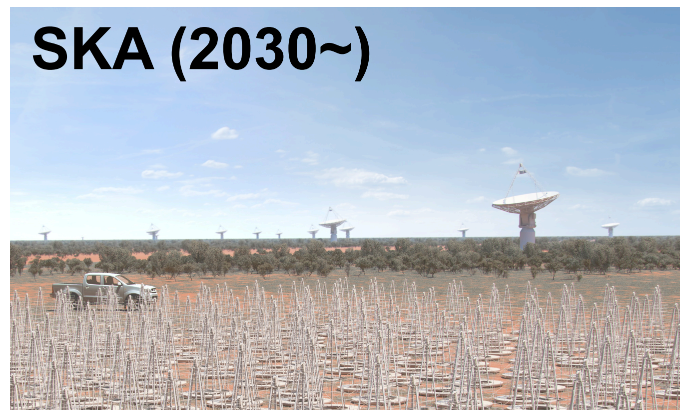

New probe of gravity!

2.7. Future detectability

S.Saga, A.Taruya, Y.Rasera, M-A.Breton (2109.06012)

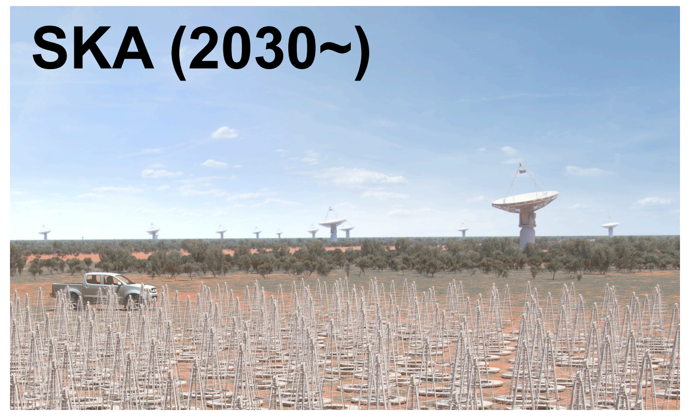

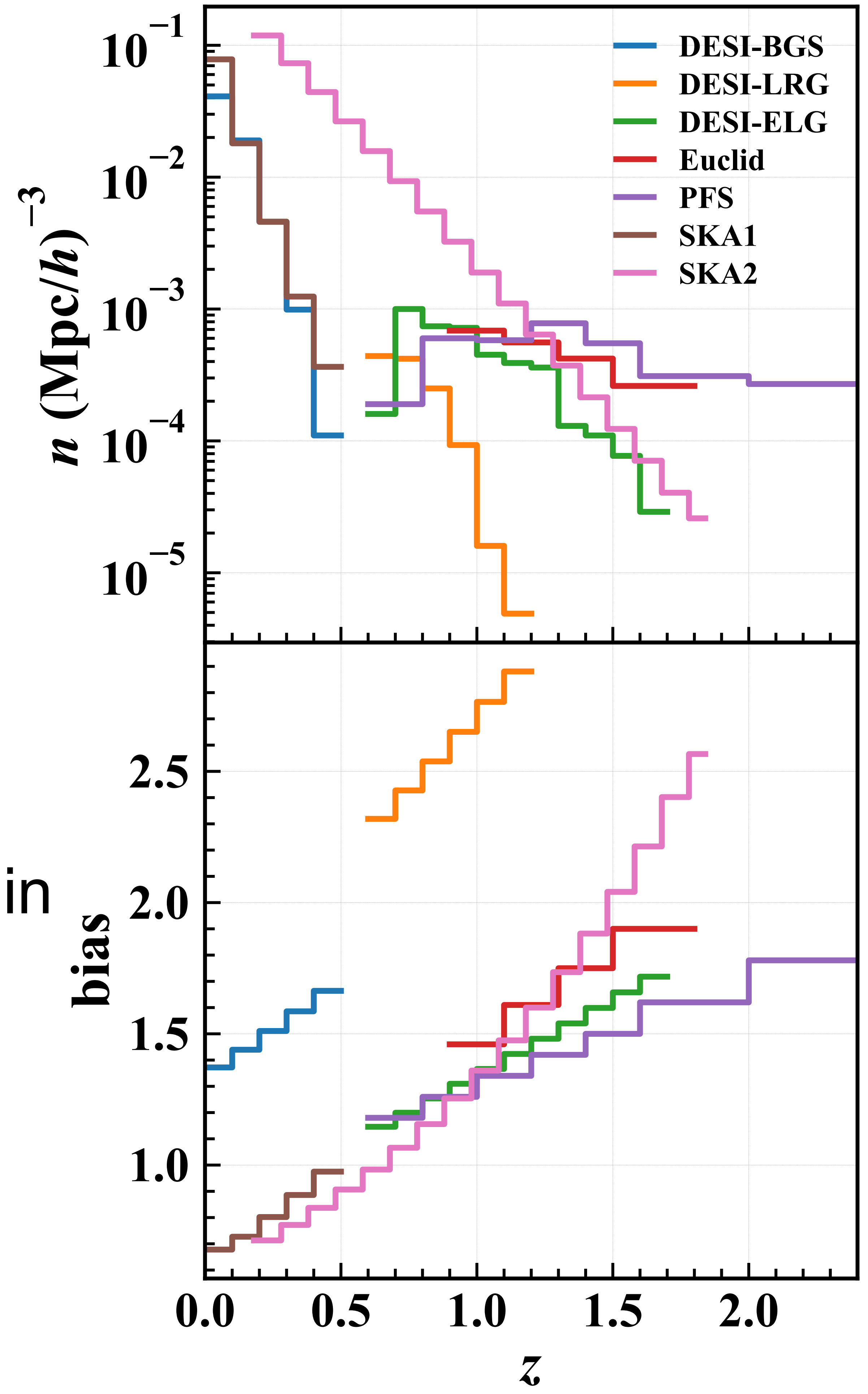

Cross-correlation between different biased objects

Strategy 1: Split a single sample into two subsamples

Assume galaxies follow the halo distribution with $M_{halo} > M_{min}$

subsample with small bias: $[M_{min}, M^*]$

subsample with large bias: $[M^*, \infty]$

The uncertainty of how M* is determined remains.

Strategy 2: Combining several types of samples from different surveys

Assume survey regions are fully overlapped

2.8. Results

S.Saga, A.Taruya, Y.Rasera, M-A.Breton (2109.06012)

Strategy 1: Split a single sample into two subsamples

Assuming galaxies follow the halo distribution with $M_{halo} > M_{min}$

subsample with small bias: $[M_{min}, M^*]$

subsample with large bias: $[M^*, \infty]$

The uncertainty of how M* is determined remains.

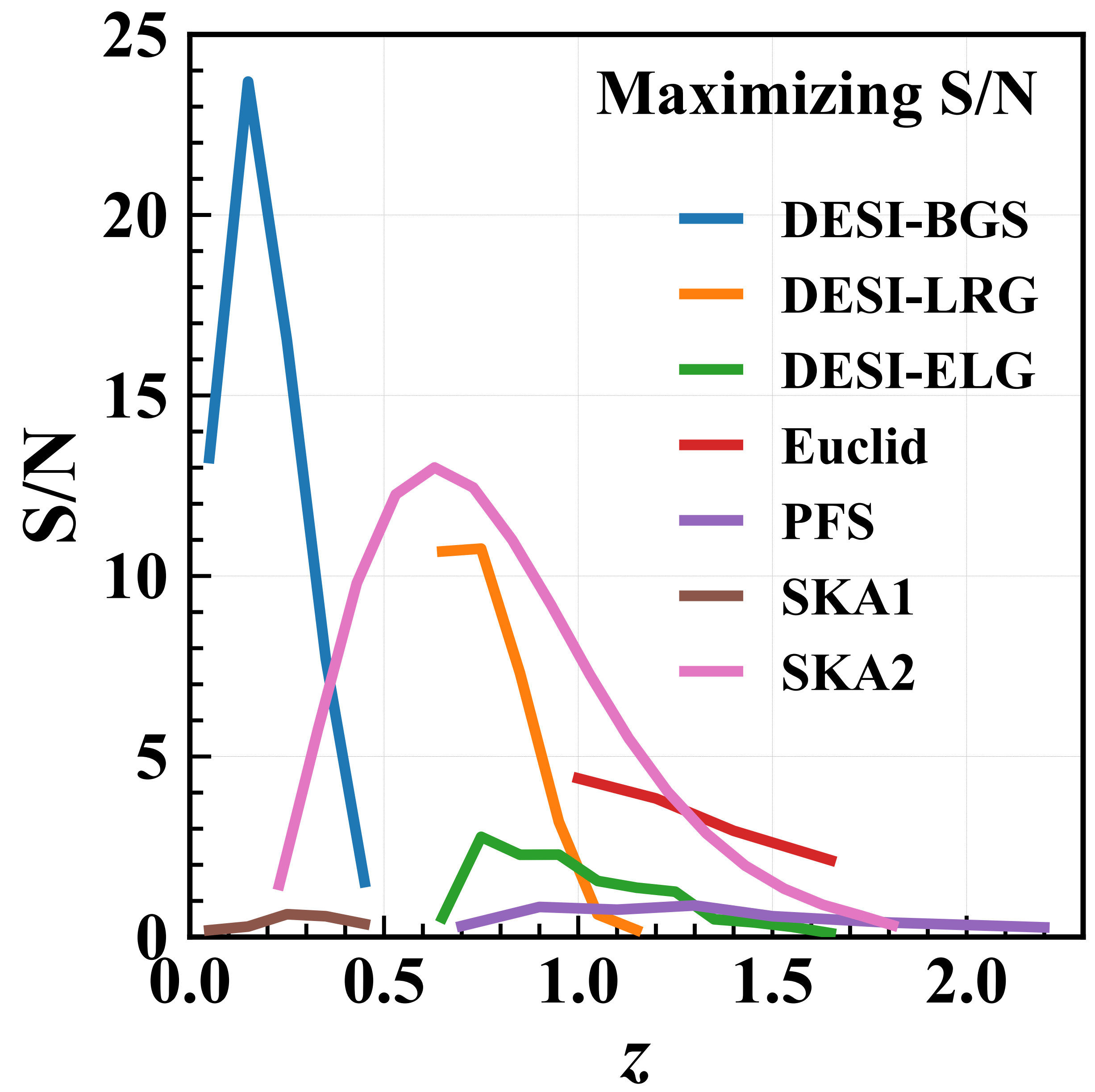

Strategy 2: Combining several types of samples from different surveys

Assuming survey regions are fully overlapped

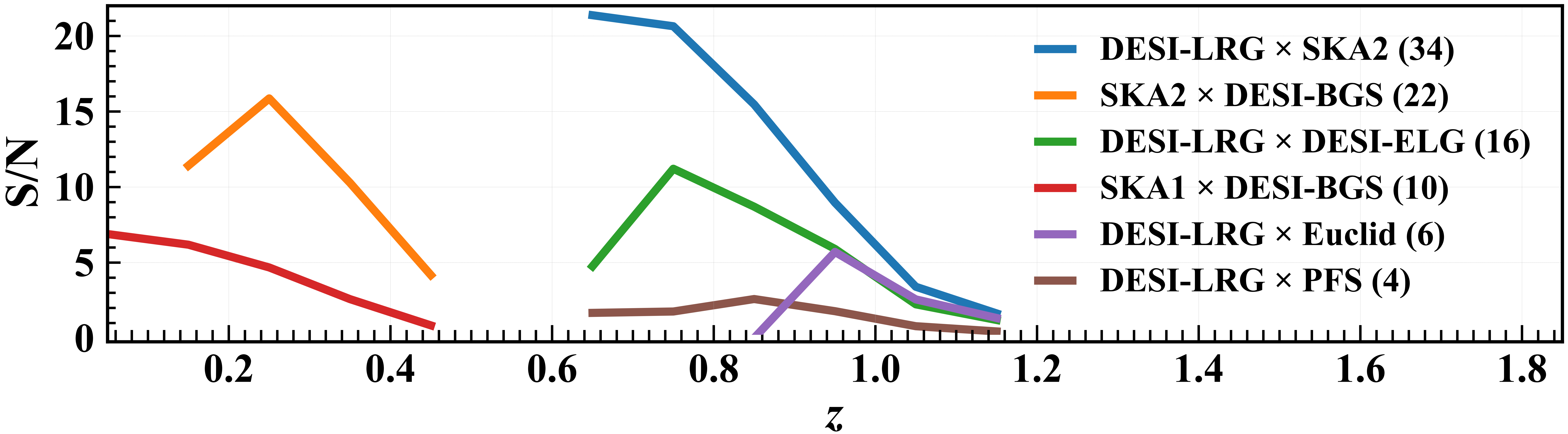

2.9. Short summary

Gravitational redshift effects(halo potential)

↓

Dipole in the galaxy-galaxy cross-correlation with **different biased objects**

↓

Future surveys can detect them with large SN~10−20!

🤔However two or more different biased samples are needed

uncertainty: how we get (sub)samples...?

cross-correlation between...

one type of biased samples & its shape information

Contents

3.1. Galaxy-Intrinsic alignment correlations

$$\xi = \langle \delta(s_1)\gamma_{+/\times}(s_2)\rangle$$

Our model **Linear alignment model**

P.Catelan et al. (2001)
C.M.Hirata & U.Seljak (2004)

Projection onto a plane perpendicular to the **(not-fixed)** line-of-sight direction:

$$\gamma^{\rm I}_{ij}(\boldsymbol{x}) = b_{\rm K}\left[\mathcal{P}_{ik}(\hat{\boldsymbol{x}})\mathcal{P}_{jl}(\hat{\boldsymbol{x}}) - \frac{1}{2}\mathcal{P}_{ij}(\hat{\boldsymbol{x}})\mathcal{P}_{kl}(\hat{\boldsymbol{x}})\right]\left(\frac{\partial_i\partial_j}{\partial^2} - \frac{1}{3}\delta_{ij}\right)\delta_{\rm L}(\boldsymbol{x})$$

$$\mathcal{P}_{ij}(\hat{\boldsymbol{x}}) \equiv \delta_{ij} - \hat{x}_i\hat{x}_j$$

Two independent components:

$$\begin{pmatrix} \gamma_+(\boldsymbol{x}) \\ \gamma_\times(\boldsymbol{x}) \end{pmatrix} = \begin{pmatrix} \hat{e}_{1i}(\hat{x})\hat{e}_{1j}(\hat{x}) - \hat{e}_{2i}(\hat{x})\hat{e}_{2j}(\hat{x}) \\ 2\hat{e}_{1i}(\hat{x})\hat{e}_{2j}(\hat{x}) \end{pmatrix}\gamma^{\rm I}_{ij}(\boldsymbol{x})$$

Coordinates:

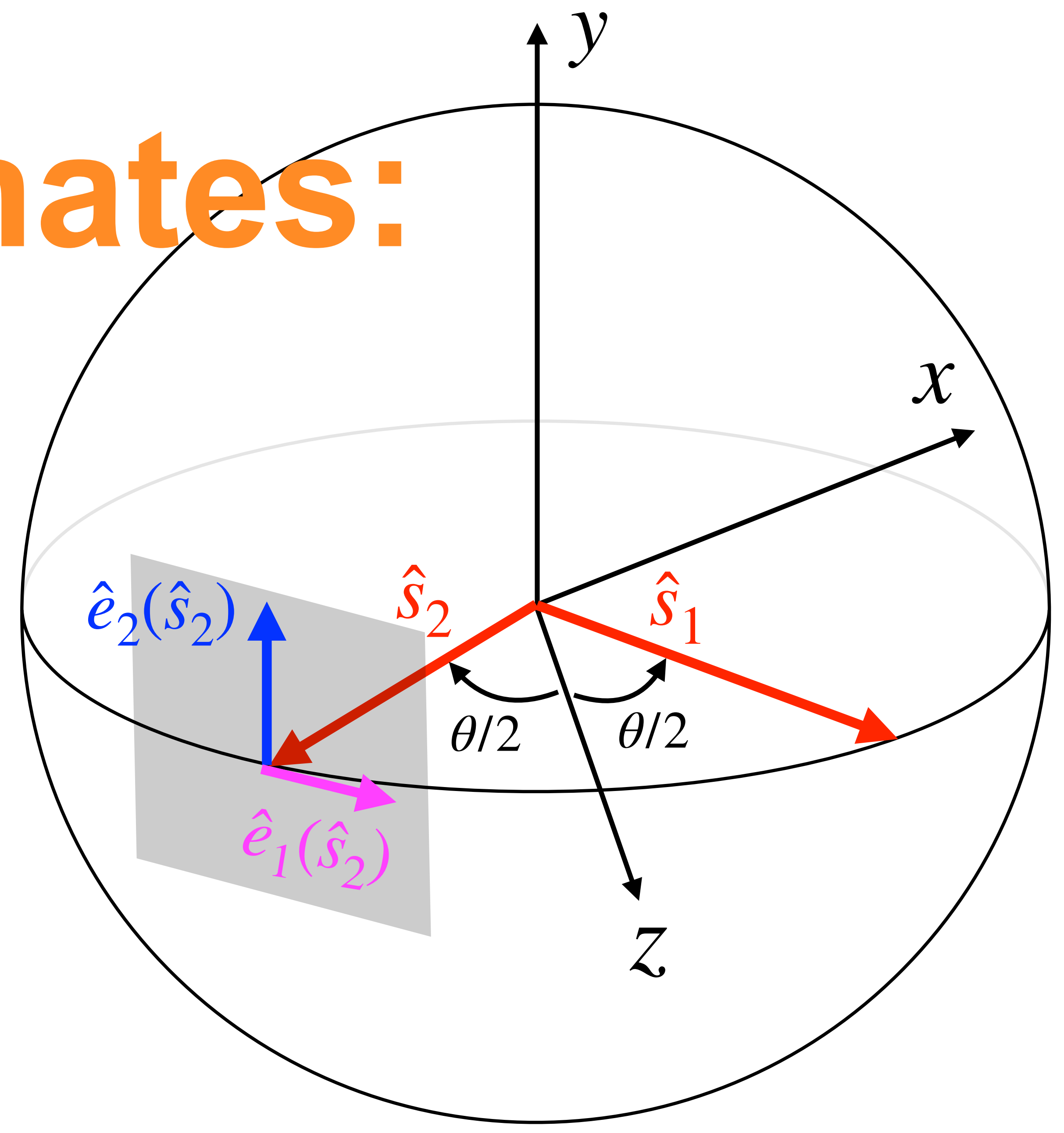

$$\langle \delta(s_1)\gamma_\times(s_2)\rangle = 0$$

3.3. Demonstration: multipole moments

$$\xi = \langle \delta(s_1)\gamma_+(s_2)\rangle = \langle \delta^{(\mathrm{std})}(s_1)\gamma_+(s_2)\rangle + \langle \delta^{(\mathrm{pot})}(s_1)\gamma_+(s_2)\rangle + \langle \delta^{(\mathrm{NL})}(s_1)\gamma_+(s_2)\rangle$$

$$\equiv \xi^{(\mathrm{std})} + \xi^{(\mathrm{pot})} + \xi^{(\mathrm{NL})}$$

$$\xi_\ell = \frac{2\ell+1}{2}\int_{-1}^{1}\left(\xi^{(\mathrm{S})}(\boldsymbol{s}_1,\boldsymbol{s}_2)\,P_\ell(\cos\theta)\right)\mathrm{d}\cos\theta$$

Our model

$\delta^{(\mathrm{std})}$ = Real space + Doppler effect

$$\equiv \int \frac{\mathrm{d}^3\boldsymbol{k}}{(2\pi)^3}\mathrm{e}^{\mathrm{i}\boldsymbol{k}\cdot\boldsymbol{s}}\left[b + f\mu_k^2 - \mathrm{i}f\frac{2}{ks}\mu_k\right]\delta_{\mathrm{L}}(\boldsymbol{k})\,,$$

$\delta^{(\mathrm{pot})}$ = Linear potential

$$\equiv \int \frac{\mathrm{d}^3\boldsymbol{k}}{(2\pi)^3}\mathrm{e}^{\mathrm{i}\boldsymbol{k}\cdot\boldsymbol{s}}\left[(iks\mu_k + 2)\,\frac{\mathcal{M}}{sk^2}\right]\delta_{\mathrm{L}}(\boldsymbol{k})\,,$$

$$\mathcal{M} \equiv -3\Omega_{\mathrm{m0}}H_0^2/(2a^2H)$$

$\delta^{(\mathrm{NL})}$ = NL potential

$$\equiv -\frac{\Phi_{\mathrm{NL}}}{aHs}\int \frac{\mathrm{d}^3\boldsymbol{k}}{(2\pi)^3}\mathrm{e}^{\mathrm{i}\boldsymbol{k}\cdot\boldsymbol{s}}\Big[-1 + (1-2f)\mu_k^2 - \mathrm{i}(1+f)\frac{2}{ks}\mu_k - \mathrm{i}bks\mu_k - \mathrm{i}fks\mu_k^3\Big]\delta_{\mathrm{L}}(\boldsymbol{k})\,,$$

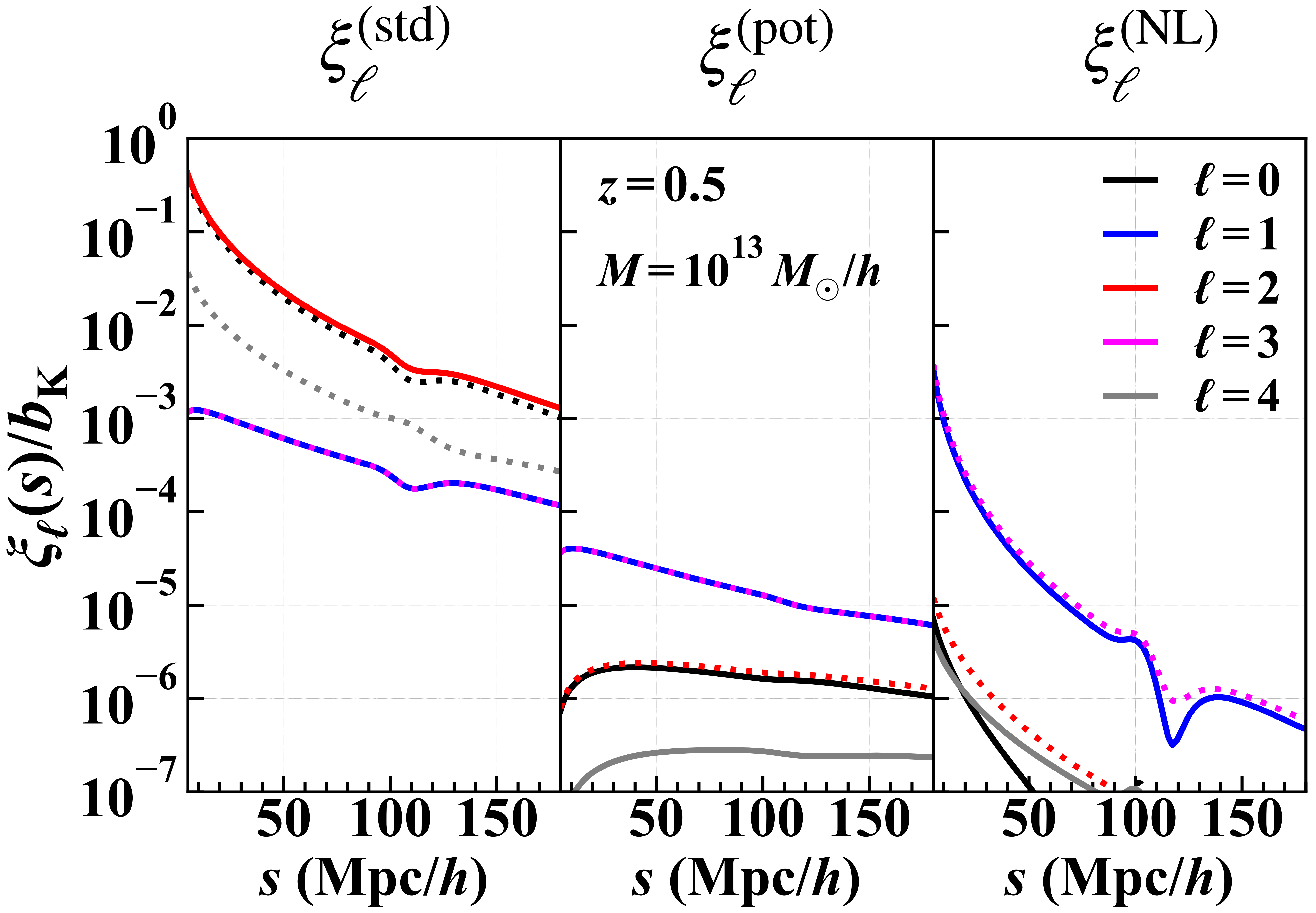

3.3. Demonstration: multipole moments

$$\xi = \langle \delta(s_1)\gamma_+(s_2)\rangle = \langle \delta^{(\mathrm{std})}(s_1)\gamma_+(s_2)\rangle + \langle \delta^{(\mathrm{pot})}(s_1)\gamma_+(s_2)\rangle + \langle \delta^{(\mathrm{NL})}(s_1)\gamma_+(s_2)\rangle$$

$$\equiv \xi^{(\mathrm{std})} + \xi^{(\mathrm{pot})} + \xi^{(\mathrm{NL})}$$

$$\xi_\ell = \frac{2\ell+1}{2}\int_{-1}^{1}\left(\xi^{(\mathrm{S})}(\boldsymbol{s}_1,\boldsymbol{s}_2)\,P_\ell(\cos\theta)\right)\mathrm{d}\cos\theta$$

Similarities with GG correlations:

- even multipoles are dominated by "std"
- wide-angle effects in "std" produce odd multipoles
- "NL" dominates small-scale odd multipoles

Difference:

- std & NL dipole are the same sign (no sign flip at small scales)

➡ **GI dipole**

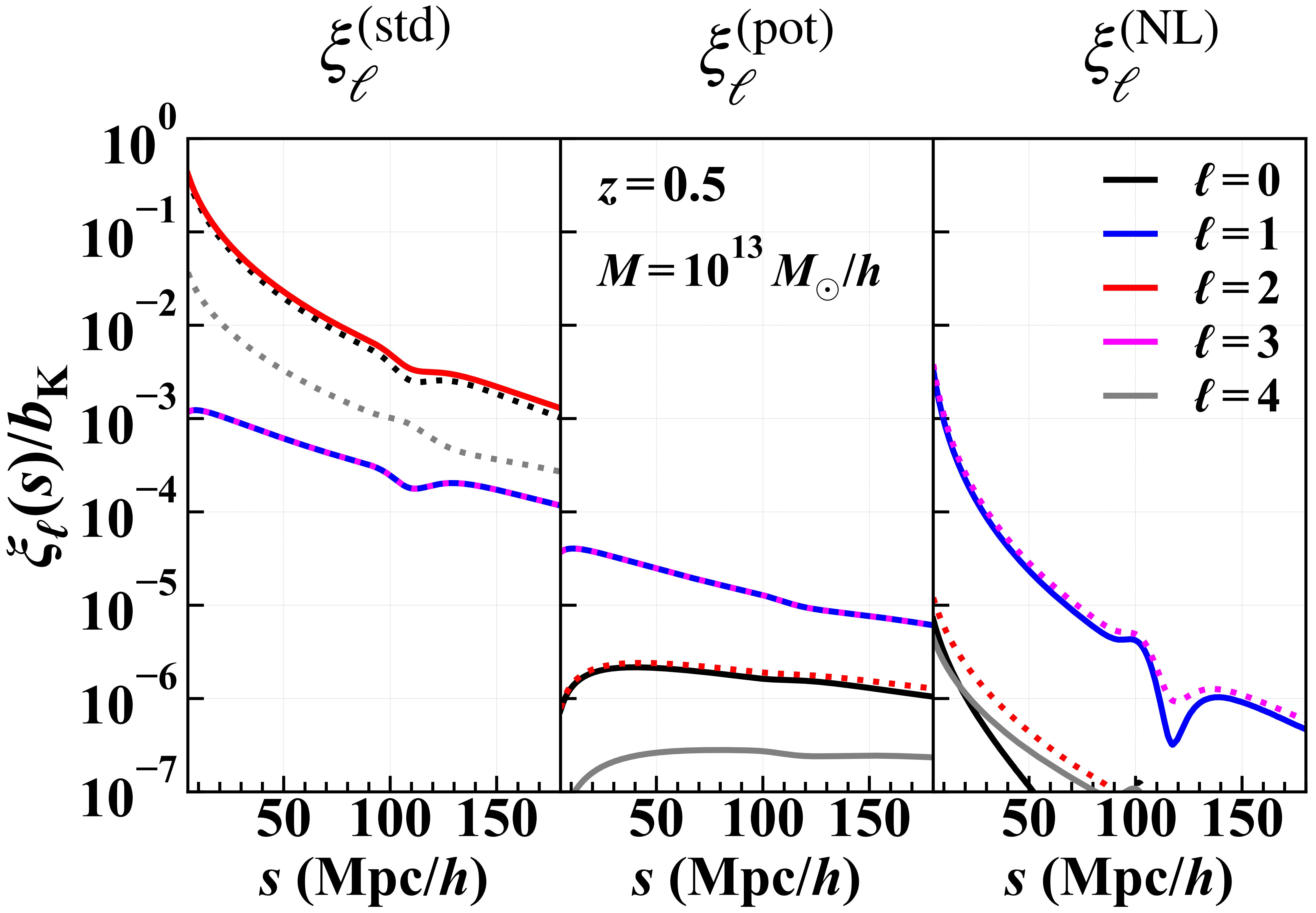

3.4. Demonstration: dipole signals

New simple formulae including **wide-angle effects & gravitational redshift effect**

$$\xi_1^{(\mathrm{std})} = \frac{2}{5}(b+f)\, b_{\mathrm{K}} \Xi_2^{(0)}$$

$$\xi_1^{(\mathrm{pot})} = -\frac{2}{5}\mathcal{M} s b_{\mathrm{K}} \Xi_3^{(1)}$$

$$\xi_1^{(\mathrm{NL})} = -\frac{2}{5}\frac{\Phi_{\mathrm{NL}}}{aHs} b_{\mathrm{K}} b \Xi_3^{(-1)} - \frac{2}{105} f \frac{\Phi_{\mathrm{NL}}}{aHs} b_{\mathrm{K}} \left(7\Xi_3^{(-1)} - 2\Xi_5^{(-1)}\right)$$

$$\mathcal{M} \equiv -3\Omega_{\mathrm{m0}} H_0^2/(2a^2 H)$$

$$\Xi_\ell^{(n)}(s) = \int \frac{k^2 \mathrm{d}k}{2\pi^2} \frac{j_\ell(ks)}{(ks)^n} P_{\mathrm{L}}(k)$$

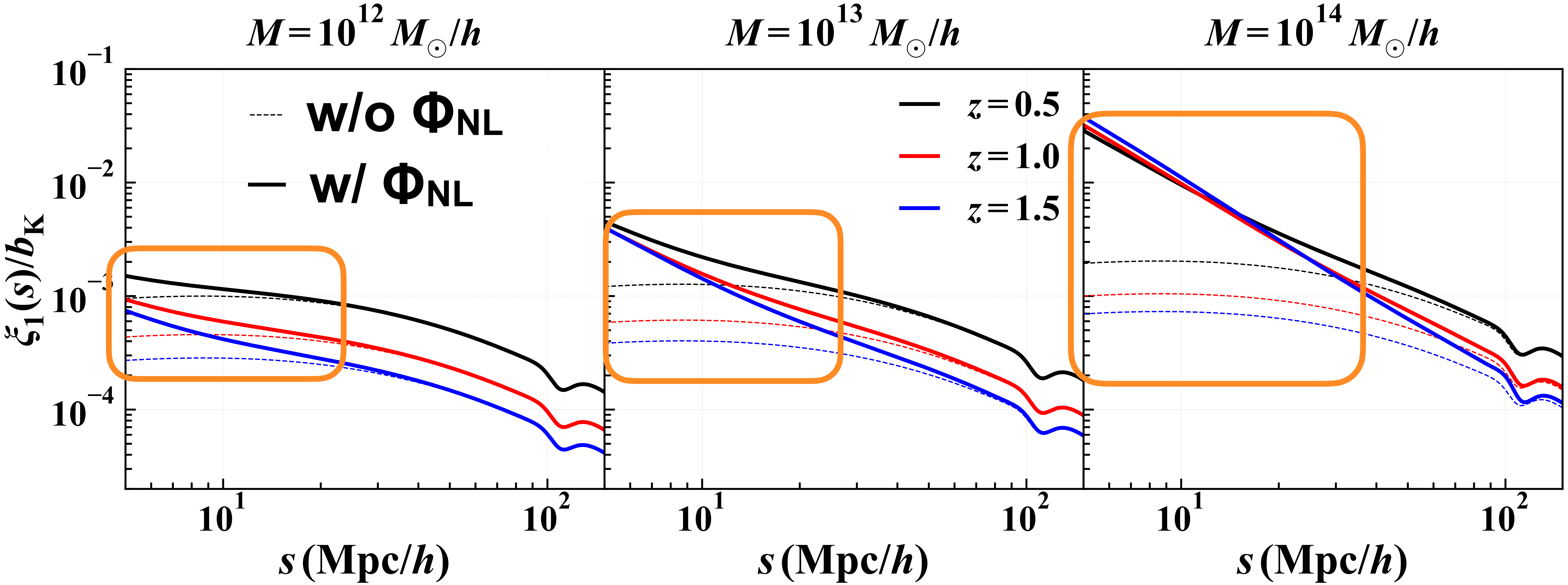

3.5. Demonstration: dipole covariance

$A_{IA} = 23$

$\sigma_{\mathrm{shape}} = 0.2$

Schematically, ...

$$\mathrm{COV}_1(s_1, s_2) \sim \frac{1}{V}\sum_{\ell,\ell'}\left(\xi^{\mathrm{gg}}_{\ell} \times \xi^{\mathrm{II}}_{\ell'} + \xi^{\mathrm{gI}}_{\ell} \times \xi^{\mathrm{gI}}_{\ell'}\right)$$

CV×CV term

$$\frac{1}{V}\sum_{\ell'}\left(\frac{1}{n_{\mathrm{g}}} \times \xi^{\mathrm{II}}_{\ell'} + \frac{\sigma^2_{\mathrm{shape}}}{n_{\mathrm{g}}} \times \xi^{\mathrm{gg}}_{\ell'}\right)$$

CV×P term

$$\frac{1}{V}\frac{1}{n_{\mathrm{g}}}\frac{\sigma^2_{\mathrm{shape}}}{n_{\mathrm{g}}}$$

P×P term

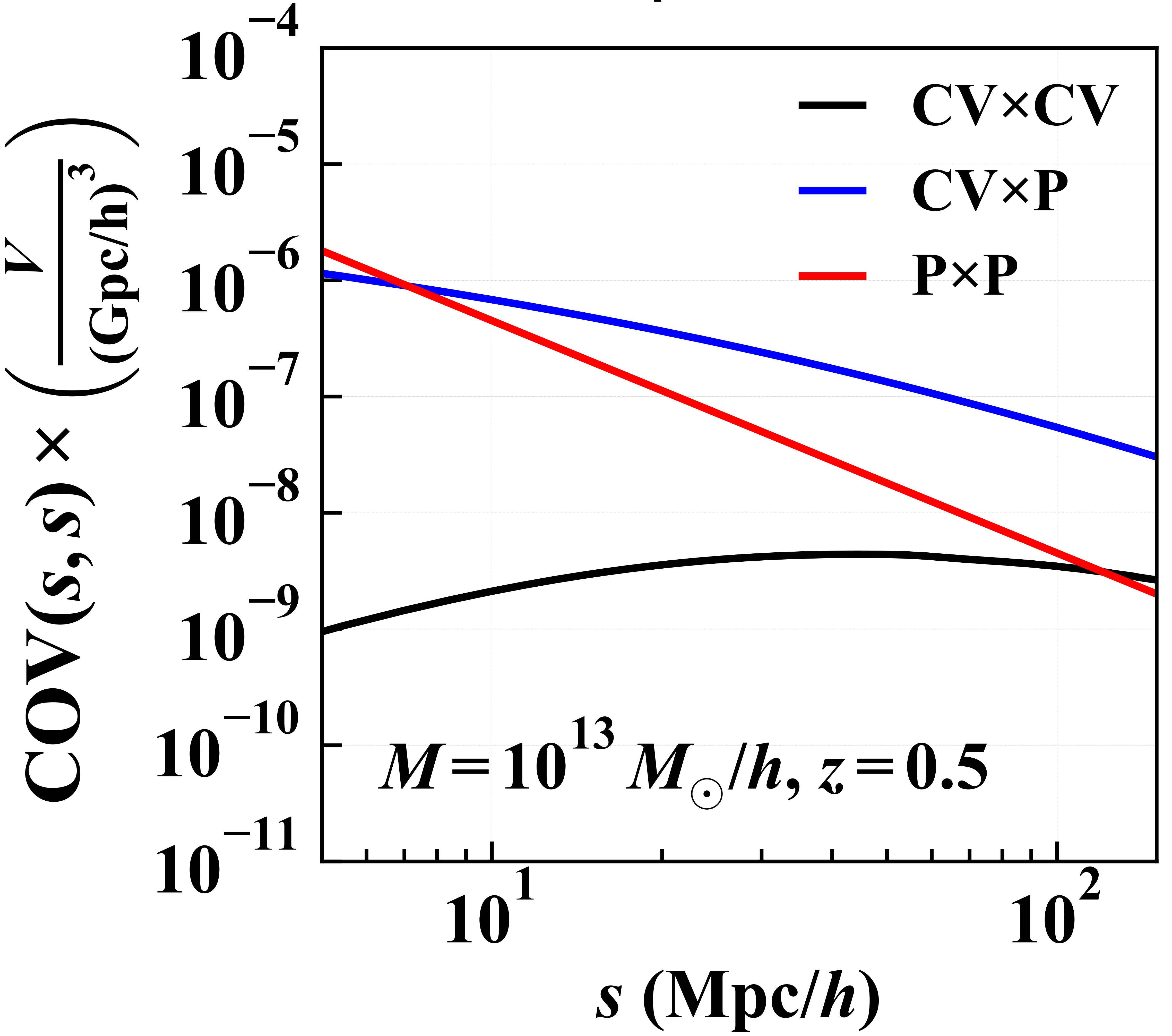

NOTE: instead using Legendre polynomial $P_\ell(\cos\theta)$, we need to carefully treat the angular dependence by using $Y_{\ell,m}(\theta,\phi)$ in computing covariance matrix.

3.6. Demonstration: signal-to-noise ratio

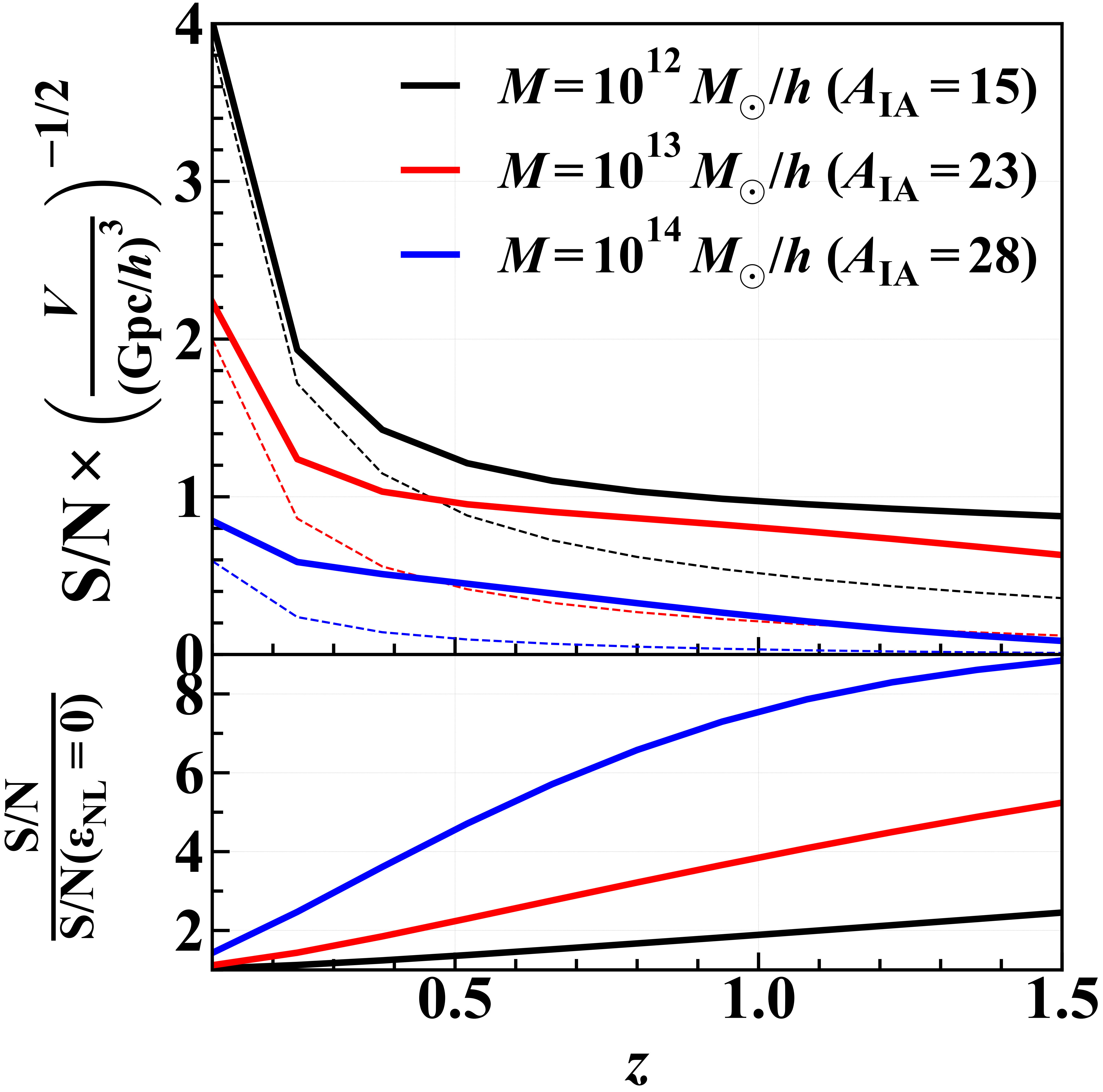

$$\left(\frac{\mathrm{S}}{\mathrm{N}}\right)^2 = \sum_{s_1,s_2=s_{\min}}^{s_{\max}} \xi_1(s_1)(\mathrm{COV}_1(s_1,s_2))^{-1}\xi_1(s_2)$$

($s_{\min}$, $s_{\max}$) = (1, 150) Mpc/h

bias&number density: Sheth&Tormen(1999)

A_{IA} is chosen to match Kurita et al.(2020)

- low-z SN is dominated by wide-angle effect
- measurements at high-z have more chances

4. Summary

The galaxy-Intrinsic alignment cross-correlation can be a new probe of gravitational redshift effects

Dipole anisotropy in galaxy-galaxy correlations

- Two populations are needed
- SN reaches ~ 10−25

S.Saga, A.Taruya, M-A.Breton, Y.Rasera [2004.03772]
S.Saga, A.Taruya, Y.Rasera, M-A.Breton [2109.06012]

Dipole anisotropy in galaxy-IA correlations:

- Single galaxy populations + shape information
- Rough estimation implies SN reaches $\lesssim 1-4 \times$ [volume in $(\mathrm{Gpc}/h)^3]^{1/2}$

SS et al, in prep.

Future prospects:

- SN for specific surveys + systematic effects
- Test of gravity theory
- Measurements in RayGalGroupSims